How to use seismological data to infer fault friction properties and stress. Methods, examples

Elisa Tinti

Istituto Nazionale di Geofisica e Vulcanologia

Roma - Italy

ISTITUTO NAZIONALE DI GEOFISICA E VULCANOLOGIA

Advanced Workshop on Earthquake Fault Mechanics: Theory, Simulation and Observations | 2-14 September 2019

The Abdus Salam International Centre for Theoretical Physics

Kinematic Modelling of a seismic event

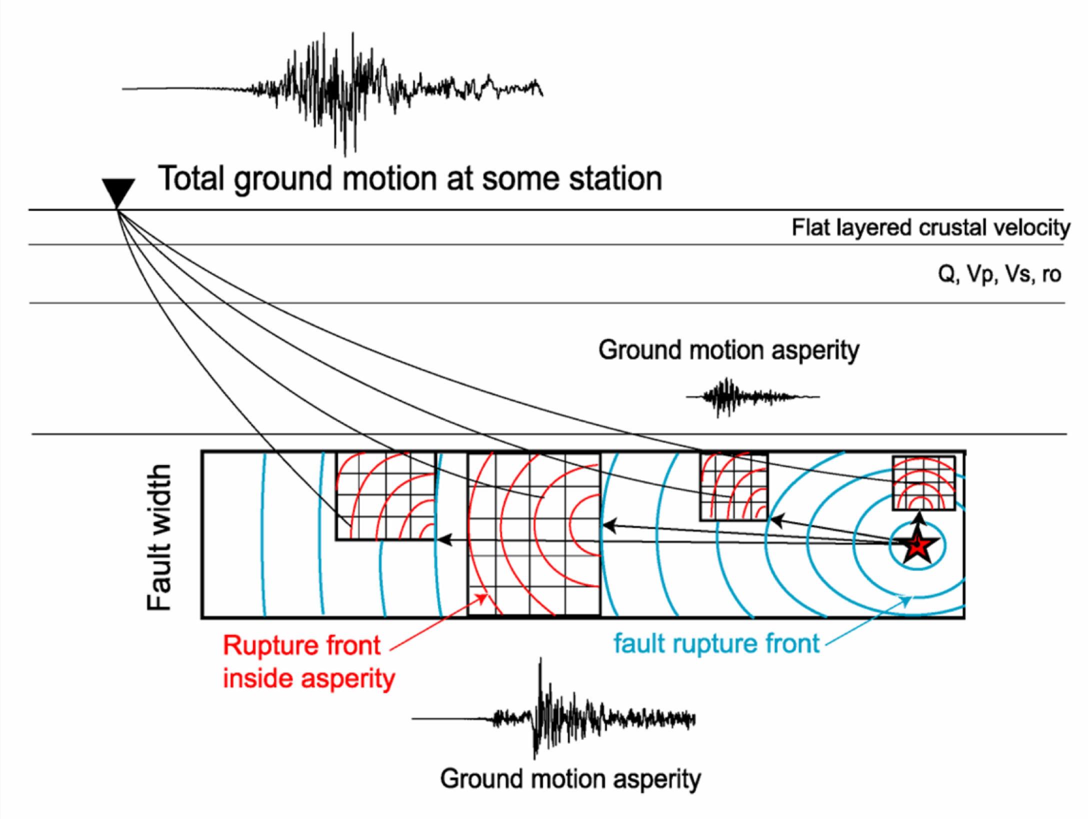

Studying the recorded waveforms at seismic stations (broadband and/or accelerometers) allows us to retrieve information on seismic source in terms of slip distribution, rupture time history, rise time, peak slip velocity…

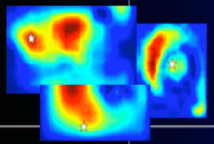

Finite-Fault Earthquake Source Model Database

SRCMOD HOME | REFERENCES | FILE FORMATS | UPLOAD | ABOUT | EQUAKE-RC HOME

username •••••••• login

Welcome to SRCMOD - an online database of finite-fault rupture models of past earthquakes!

- **Join us in our efforts to collect and disseminate earthquake rupture models by using this database for your research, contributing your rupture models that you obtain(ed) in your research, and sending us comments and suggestions.**
- You can acccess the models, by searching based on meta information or browse **all the models** .
- In the list of the models, link to the page for each source model is provided under the **author** field.
- The page for each source model provide the fundamental parameters, image of slip on the fault, and download links.
- See File Formats page for details on the conventions used for MATLAB-binaries and ASCII-file formatting.
- **Your contributions to this database are highly appreciated!** We hope that the number of source models will increase as researchers send us their inversion/modeling results, not only for recent, but also for past earthquakes.
- We encourage contributors to prepare their source models in *mat-format .
- **You can download all the models (.zip files).**
- Currently: the database has **351 models from 181 earthquakes, last updated: July 16, 2019.**
- You can upload the data directly by using Upload tool.
- Please send us your inquiries and suggestions. If you discover inconsistency or error, please inform us immediately.
- **Check out the 2014 paper in the Seismological Research Letters (including an erratum).**

List all models or use the form to search

Date range (yyyy-mm-dd)
From 1906-04-18 To 2019-09-06

Magnitude range
0.0 ≤ Mw ≤ 10.0

Location
Latitude (°N): -90.0 To 90.0
Longitude (°E): -180 To 180

Depth range (km)
From 0.0 To 1000.0

Submit

Literature

2016 Amatrice, Italy Mw=6.1

Liu et al 2017

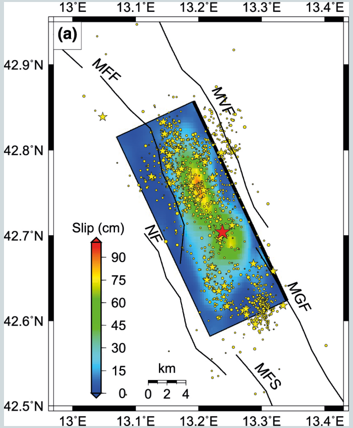

Tinti et al. 2016

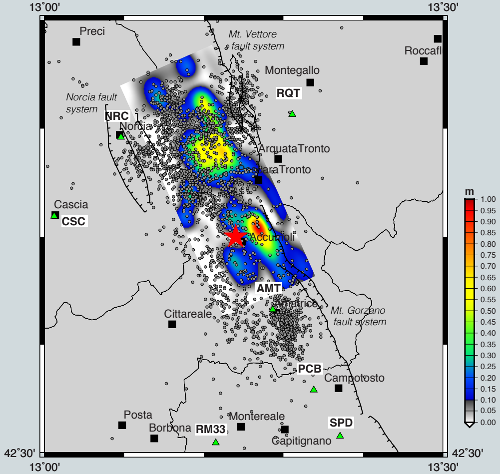

Pizzi et al. 2017

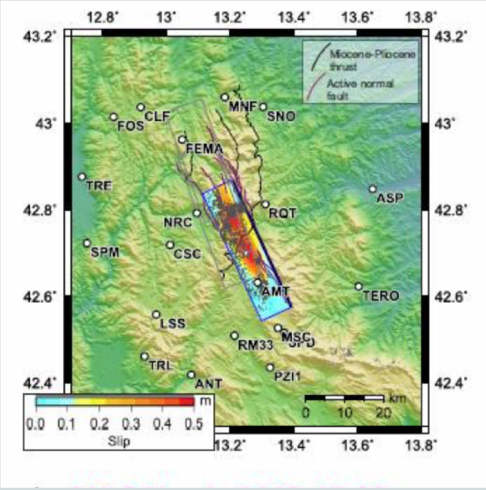

Cheloni et al 2017

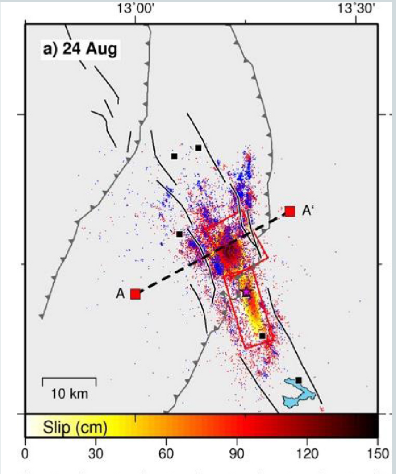

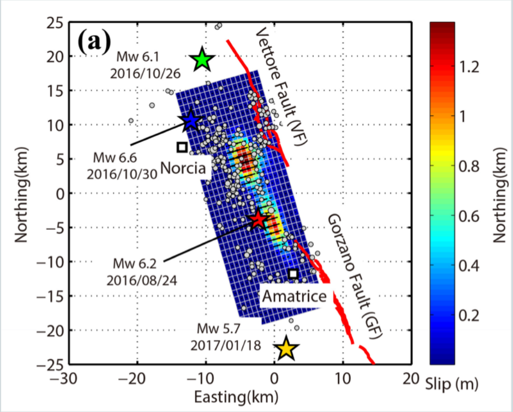

Xu et al. 2017

Lavecchia et al 2016

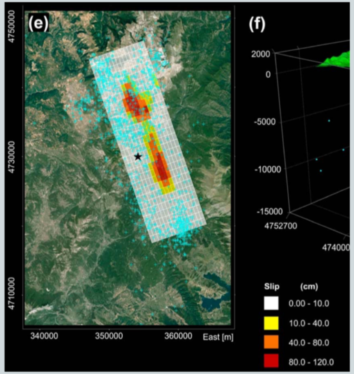

Huang et al 2017

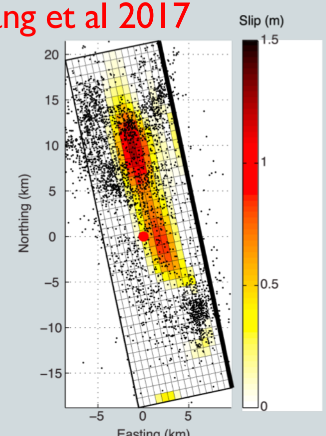

Literature

2016 Norcia (Italy) earthquake M_w 6.5

GPS horizontal and vertical displacement (red= synthetic; black= recorded)

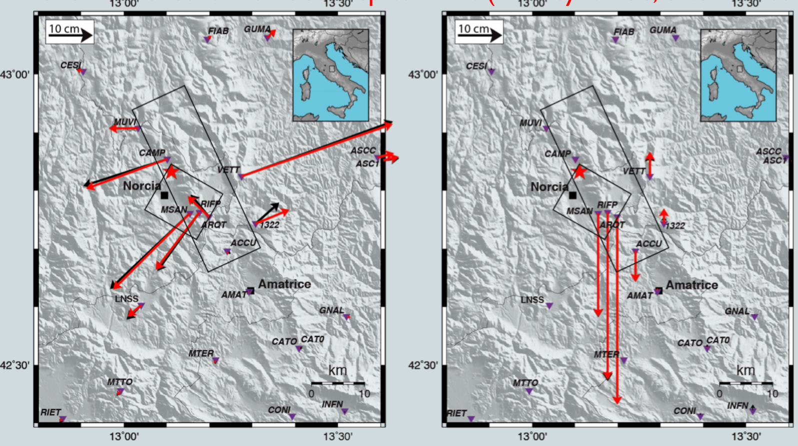

Example of a kinematic model inferred with a joint inversion of Strong motion and GPS data

Synthetic (red lines) and recorded velocity ground motions (black lines) filtered between 0.02 and 0.5 Hz

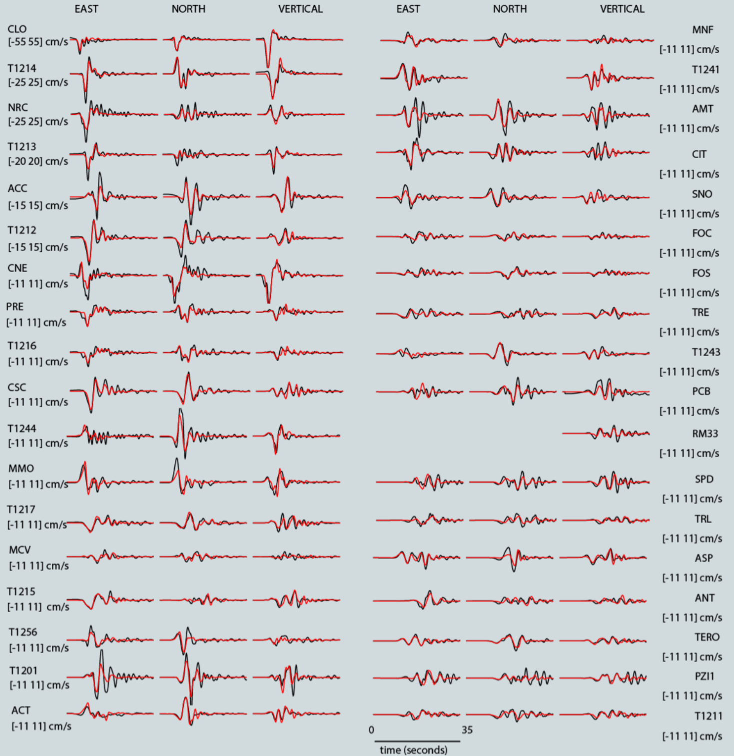

Map of SM and GPS stations

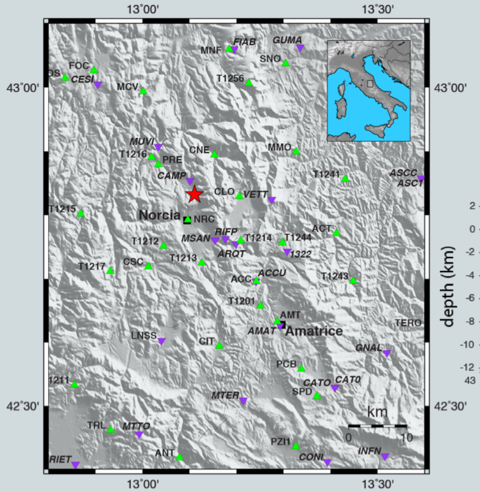

Slip distribution (3D view)

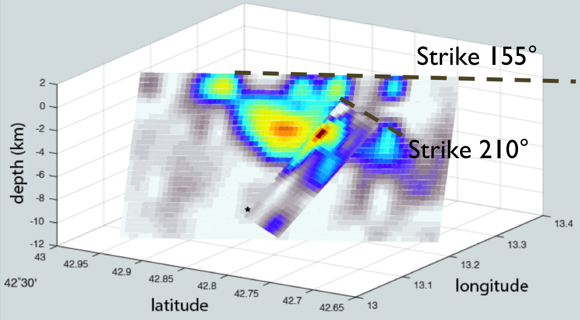

Using the representation theorem, the displacement field can be written:

$$u_i(x,t) = \boxed{\int d\tau \int_V G_{ij} f_j \, dV} + \boxed{\frac{\partial}{\partial x_q} \int d\tau \int_\Sigma [C_{jkpq} G_{ip} u_j n_k] \, dS} + \boxed{\int d\tau \int_\Sigma [G_{ip} T_p] \, dS}$$

Volume forces

Displacement on the fault plane

Traction on the fault plane

The component i of the displacement at time t in the position x is given by the contribution of:

- volume forces applied to the body;
- contribution of the displacement on the surface S (where there is the discontinuity);
- traction contribution on the surface S (within the considered volume)

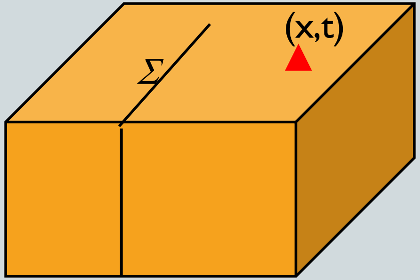

- To solve this equation we need boundary conditions!

$$u_i(x,t) = \int d\tau \int_V G_{ij} f_j dV + \frac{\partial}{\partial x_q} \int d\tau \int_\Sigma [C_{jkpq} G_{ip} u_j n_k] dS + \int d\tau \int_\Sigma [G_{ip} T_p] dS$$

<u>Kinematic solution</u>

<u>Dynamic solution</u>

Kynematic solution

The most widely used models are dislocation models in which the earthquake is represented by a displacement discontinuity along a fault plane. This representation defines a *kinematic source model*, in which the deformations on the earth are derived from an assumed slip vector that represents the inelastic displacement of the two sides of a fault.

Boundary condition: continuity of traction and discontinuity of the displacement on the fracture surface

$$u_i(x,t) = \int d\tau \int_{\Sigma} C_{jkpq} G_{ip,q} \Delta u_j n_k dS$$

The discontinuity of the displacement on the surface plane (dislocation) and the geometry of the surface are sufficient to determine the displacement in all points of the medium.

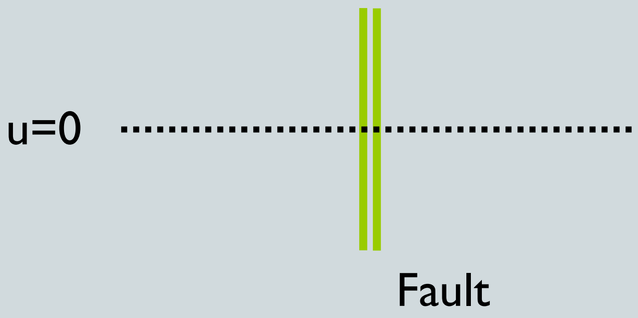

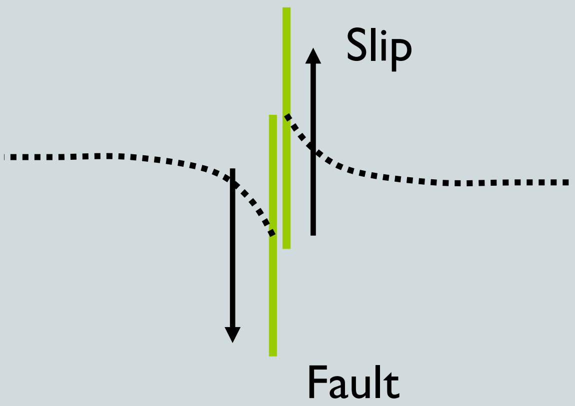

Kinematic source models and waveform modeling

Input

Strong motion waveform

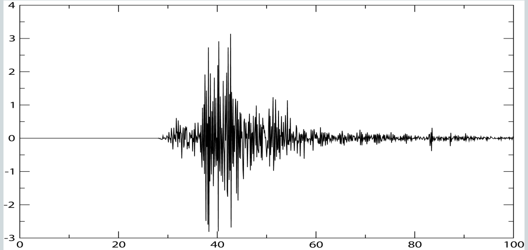

Kinematic inversion procedure

Output

slip distribution on the fault; rupture time distribution; slip velocity time history

Slip and rupture time distribution

$\Delta u(\xi)$

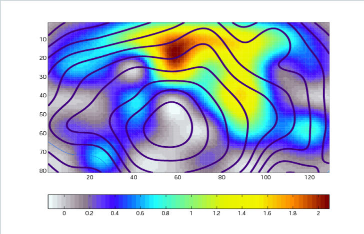

Slip velocity time history

Multi window $\Delta \dot{u}(\xi, t)$

Single window $\Delta \dot{u}(\xi, t) = \dot{f}(t - t_r(\xi)) \cdot d(\xi)$

Example: slip velocity evolution for the 1992 Landers event.

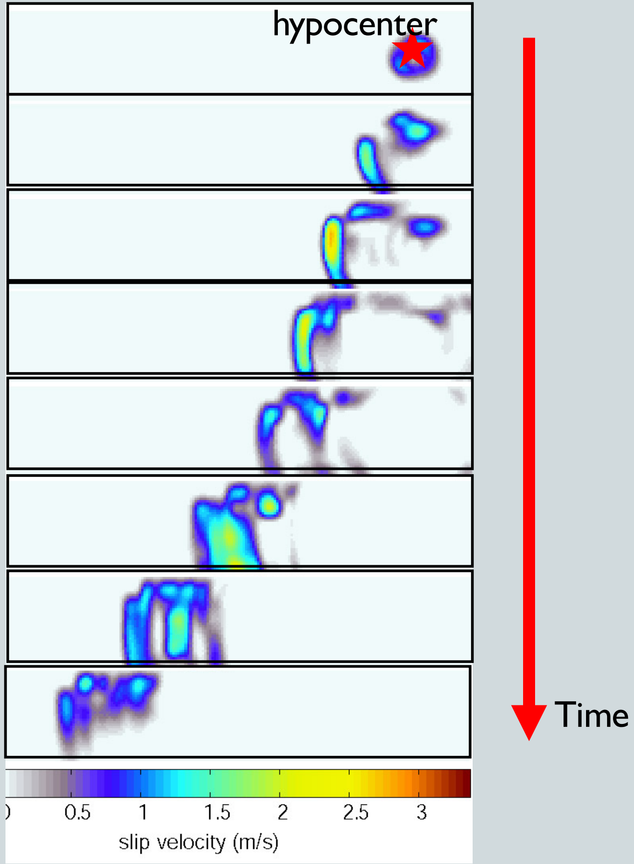

Example: slip velocity evolution and slip distribution for the 2016 M=6.5 Norcia event

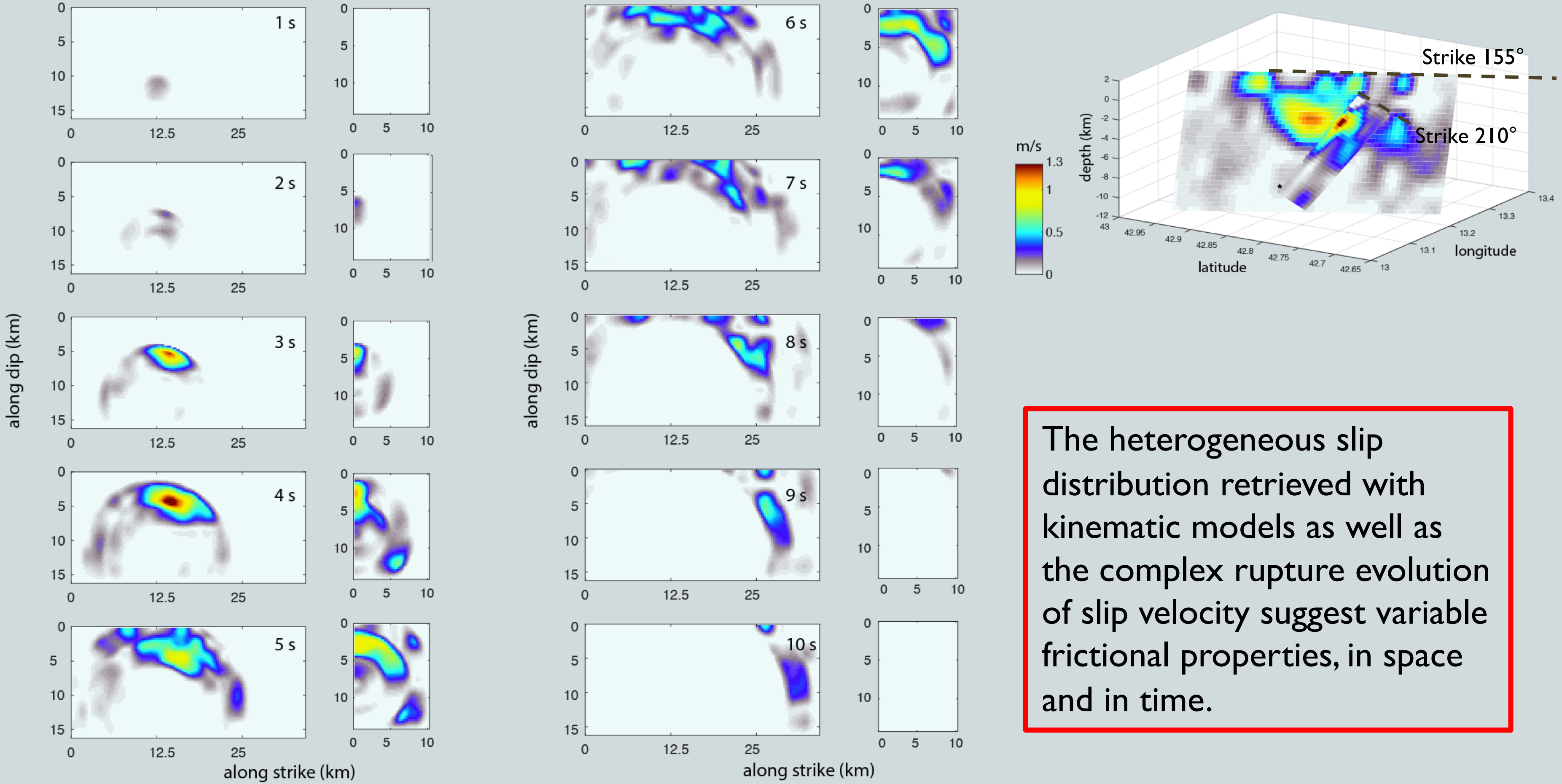

The heterogeneous slip distribution retrieved with kinematic models as well as the complex rupture evolution of slip velocity suggest variable frictional properties, in space and in time.

How can we use seismological data and these kinematic models to infer fault friction properties and stress?
Are kinematic models consistent with spontaneous dynamic ruptures?

Dynamic solution

Earthquake source dynamics provides basis for understanding the physics of earthquake initiation, propagation and arrest of an event. The *dynamic source model* describes the seismic source as a propagating shear fracture due to an initial stress field. In the dynamic approach the dislocation is a consequence of the stress conditions of the rocks on the earth crust.

The main assumption in the dynamic description of seismic source is that traction across the fault is related to slip at the same point through a friction law (because the elastic condition – Hooke's law - fails on the fault plane).

Dynamic solution

Dynamic models describe the seismic source as a shear fracture/shear sliding that propagates under an initial stress field σ_{ij}^0.

Analytical solution for an isotropic and homogeneous elastic half-space

$$u_n(x_1, x_2, t) = \int d\tau \int_\Sigma G_{n\alpha} \sigma^p_{\alpha 3} dS$$

$\sigma^p_{\alpha 3}$ Shear component of the Stress tensor

$n=1,2,3$; $\alpha = 1,2$

Boundary condition: a friction law is imposed on the fault surface

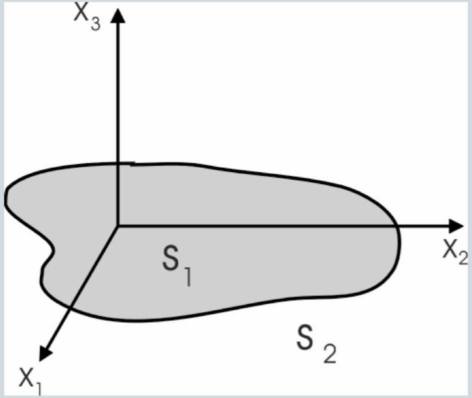

The material surrounding the fracture surface remains linearly elastic. This assumption implies that the inelastic zone is sufficiently small to be considered physically infinitesimal and to be incorporated into the fracture surface. This is the reason why most of the proposed friction laws are function of slip and slip velocity and not of strain and strain rate.

Literature

In the literature there are many dynamic models from:

- laboratory experiments
- theoretical studies
- real events.

Literature

Laboratory experiments

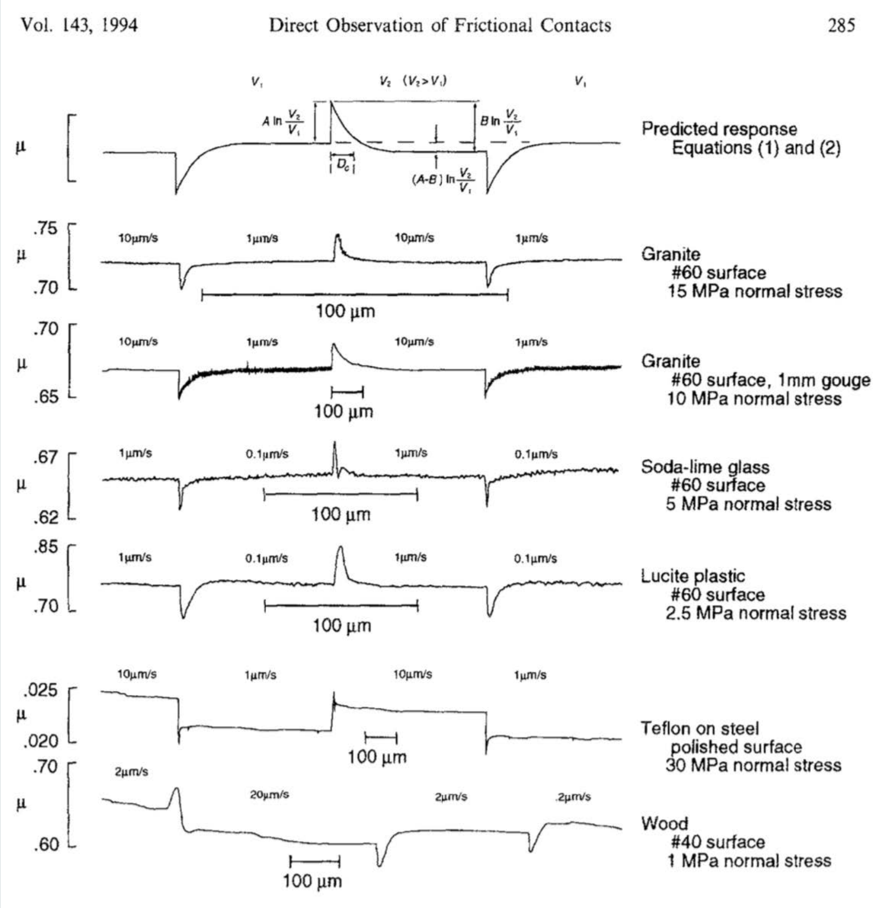

Dieterich and Kilgore 1994

For many materials:

- friction varies systematically with sliding velocity and
- exhibits transient response when velocity is changes

Rate and State friction laws were retrieved (Dieterich 1972 , Ruina 1983, …) from similar experiments. Parameters *a, b, L* can be inferred for different materials.

Literature

Laboratory experiments

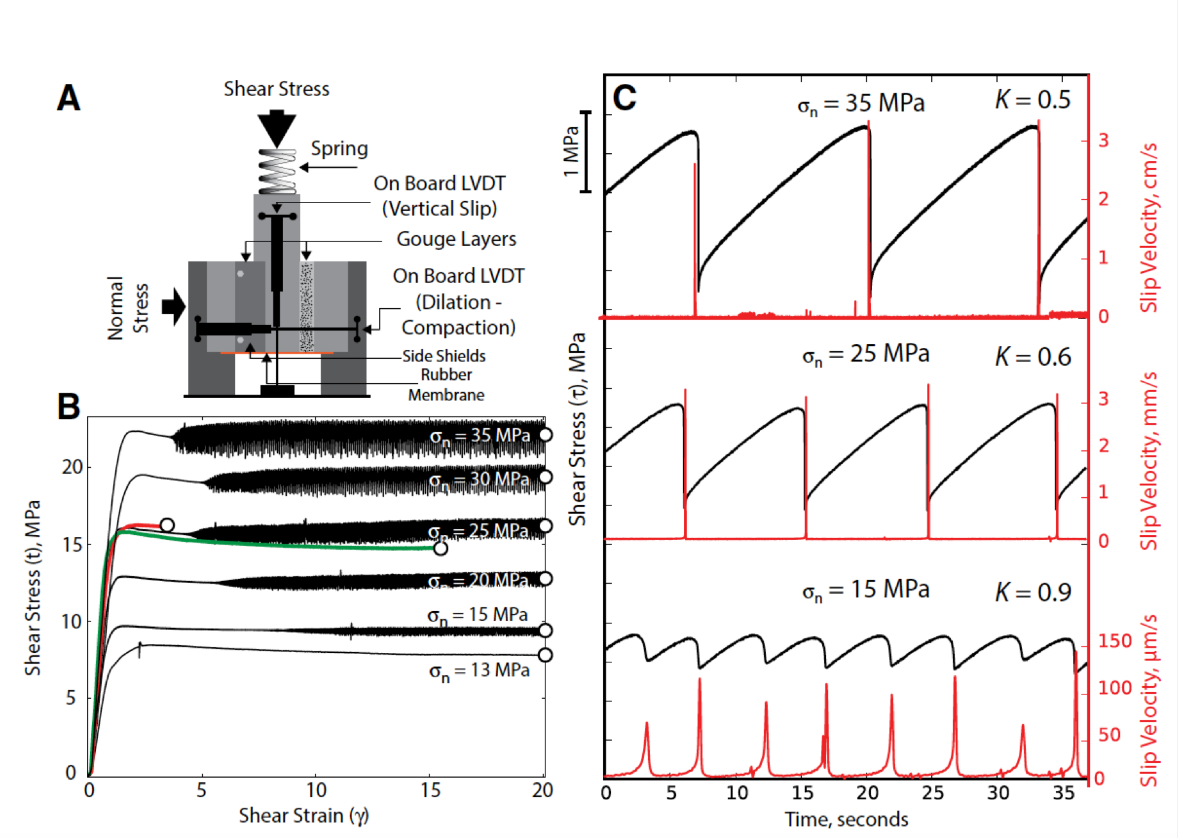

Example of seismic cycles in a velocity weakening regime at different normal stresses during the shear sliding of the gouge (Scuderi et al. 2018)

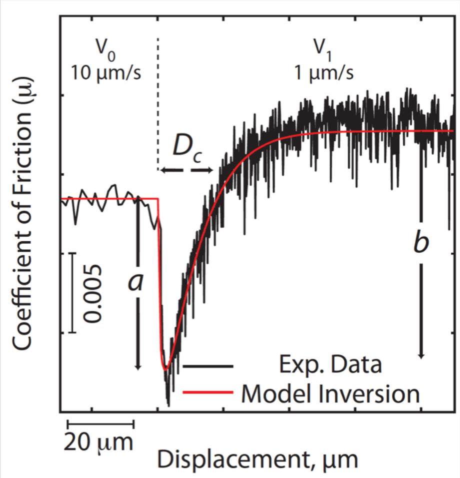

Imposing different velocity steps during the frictional sliding they observe and fit the traction evolution predicted by the rate and state friction law.

Literature

Laboratory experiments

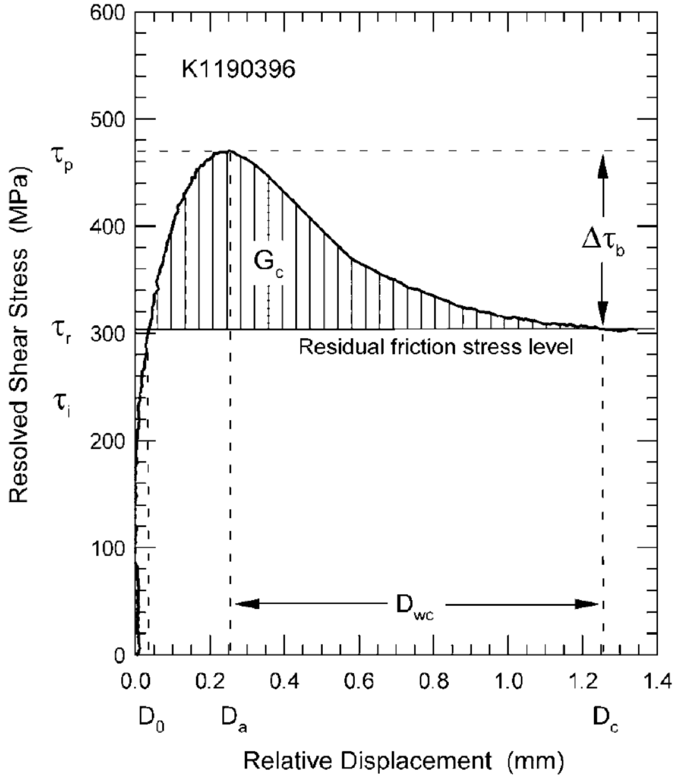

Figure 4. A typical example of the slip-dependent constitutive relation observed for the shear fracture of intact Tsukuba granite. Here τ_i is the critical stress above which

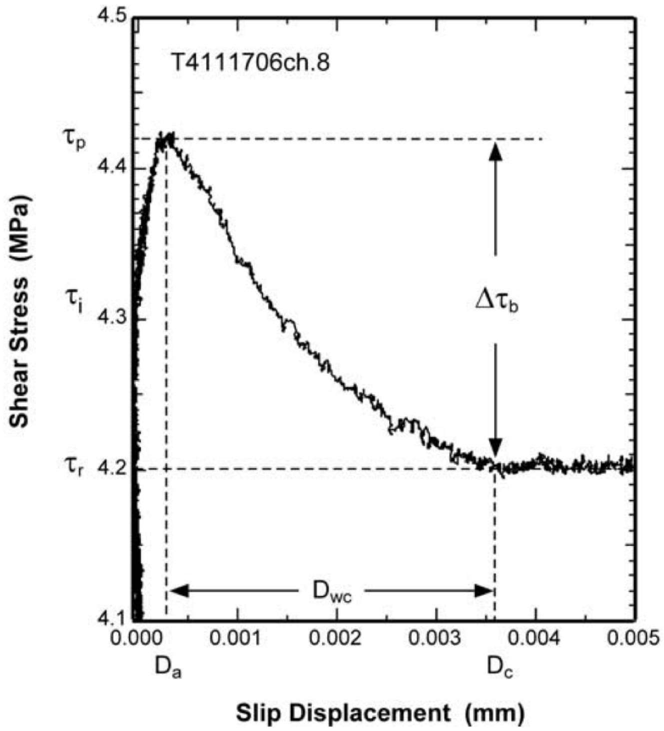

Figure 6. A typical example of the slip-dependent constitutive relation observed during the nucleation of a frictional slip failure event that proceeded slowly on a pre-cut fault whose surfaces have the characteristic length λ_c = 200 μm. Here τ_i is the critical stress above which the shear stress

Ohnaka 2003
Experiment on intact rock and pre-cut samples

Literature

Laboratory experiments

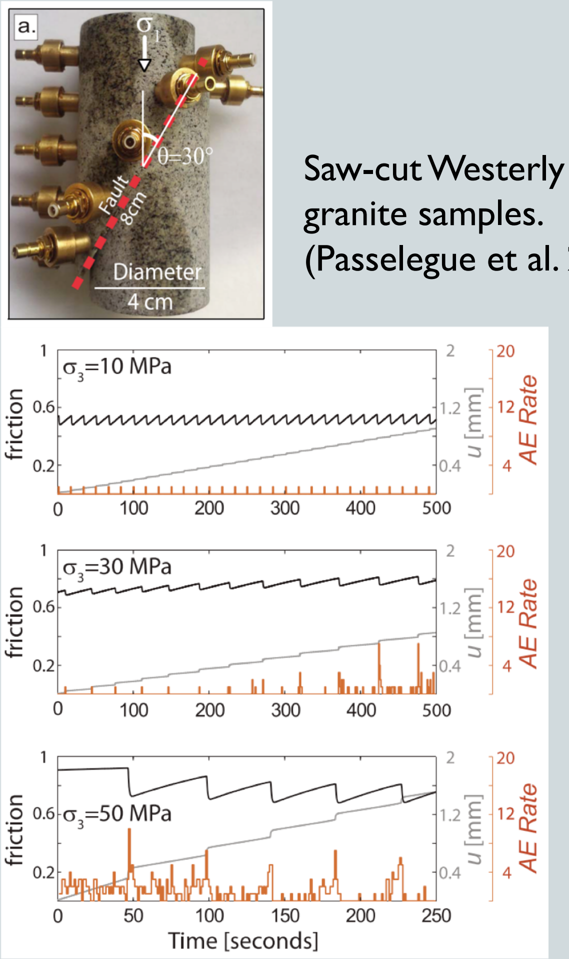

Saw-cut Westerly granite samples. (Passelegue et al. 2016)

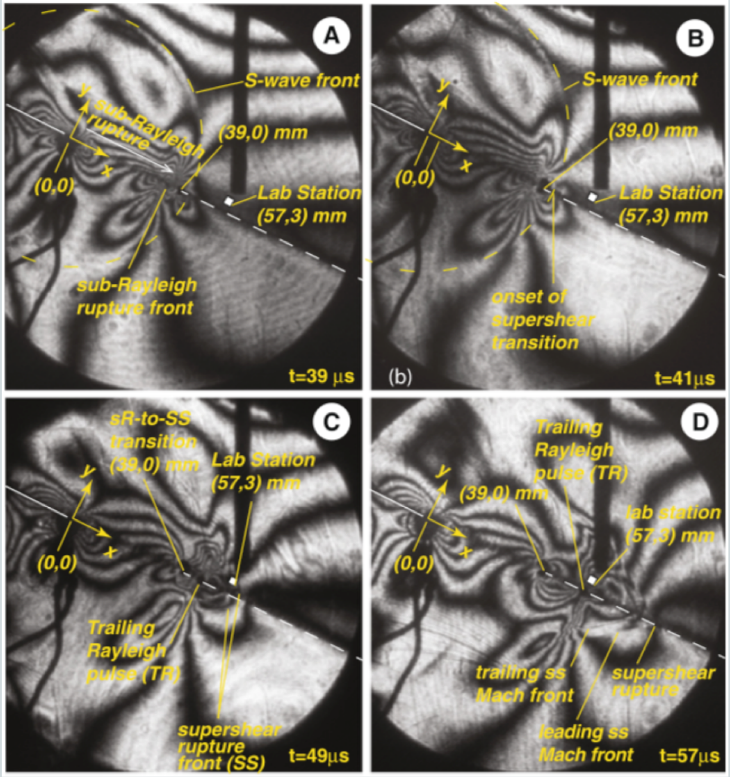

Laboratory earthquake experiments conducted using a Homalite specimen assemblies featuring a 3D fault geometry and a fault oriented at 64° with respect to the direction of the compressive principal stress.

These pictures show high-speed photoelastic images (where the fringes correspond to contours of maximum shear stress change in the medium)

Rosakis et al.

Literature

Noda and Lapusta 2013, NatGeo

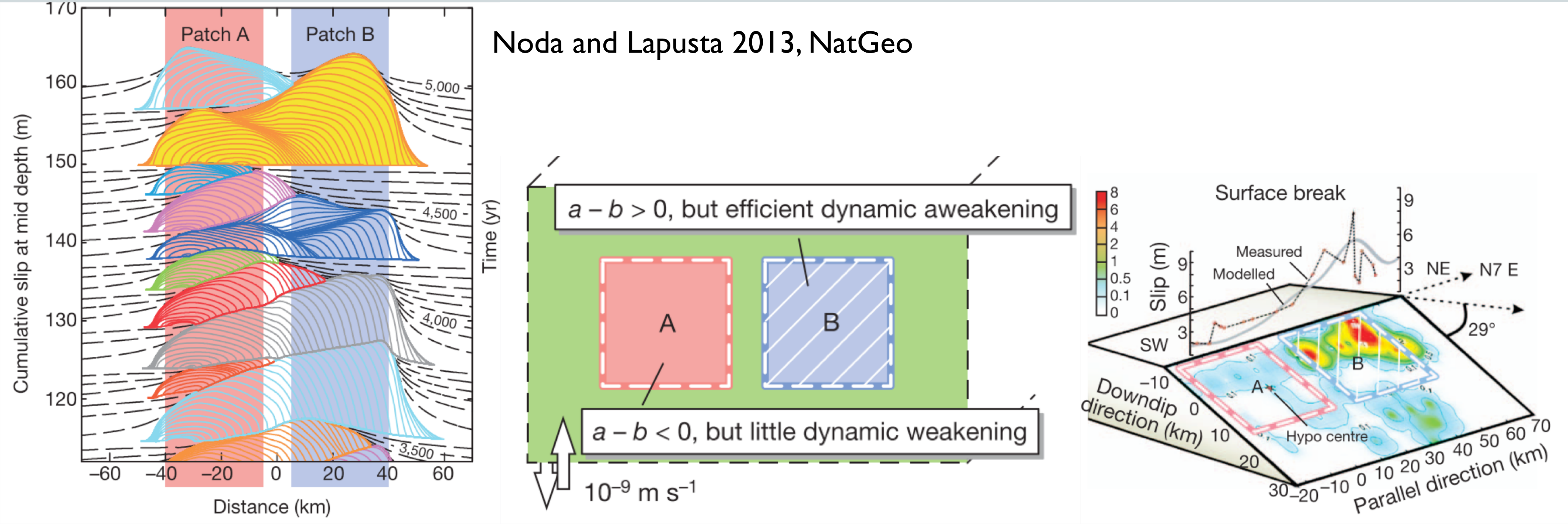

Heterogeneous conditions to reproduce
2011 Tohoku-Oki earthquake

Literature

Real events

Peyrat et al 2001

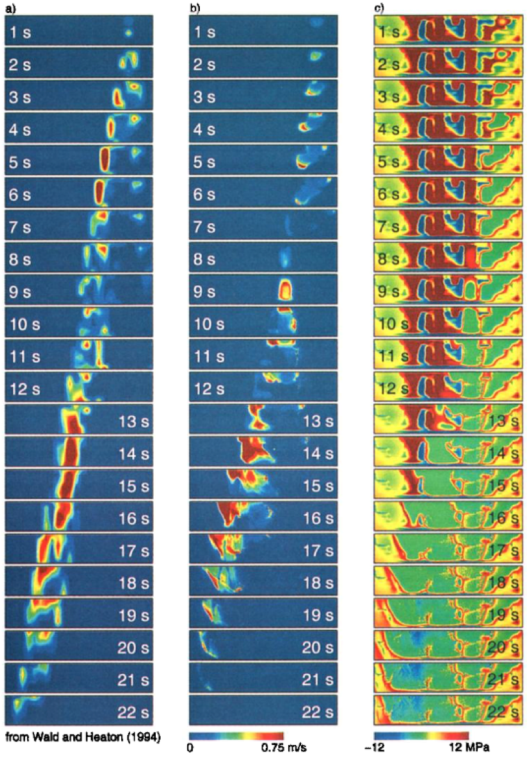

Plate 2. Snapshots of (a) the kinematic model recomputed from *Wald and Heaton* [1994] compared to (b) our dynamic rupture simulation of the 1992 Landers earthquake on the fault plane. The snapshots depict the horizontal slip rate in 1 s time slices. (c) Shear stress on the Landers fault as a function of time for our preferred dynamic rupture model described in Plate 2b. The propagation is associated with a stress decrease (green), and the rupture only propagates in regions of high stress (red).

Ulrich et al 2019

nature COMMUNICATIONS

ARTICLE

https://doi.org/10.1038/s41467-019-09125-w OPEN

Dynamic viability of the 2016 Mw 7.8 Kaikōura earthquake cascade on weak crustal faults

Thomas Ulrich[1], Alice-Agnes Gabriel[1], Jean-Paul Ampuero[2,3] & Wenbin Xu[4]

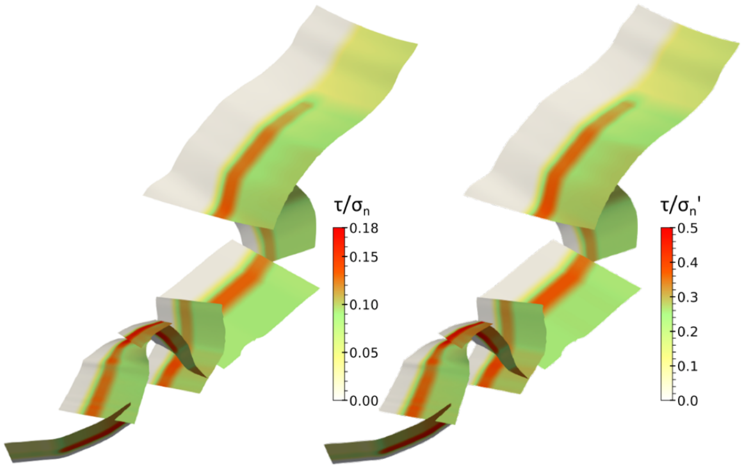

Limitation of dynamic models

1. Constitutive laws have been derived from laboratory experiments, proposed in theoretical studies and used in numerical simulations. However, there are still uncertainties about the parameters scaling to real fault dimensions: which are the actual values of dynamic parameters?
2. Limited frequency band: Usually kinematic models of extended source are inferred inverting data at frequency < 1 Hz to avoid site effects and too complex propagation effects. This limitation affects mainly the knowledge of slip velocity and the description of the processes occurring during the cohesive zone.
3. Trade-off among many kinematic and dynamic parameters

Bulletin of the Seismological Society of America, 90, 1, pp. 98–116, February 2000

What Can Strong-Motion Data Tell Us about Slip-Weakening Fault-Friction Laws?

by Mariagiovanna Guatteri and Paul Spudich

Abstract We consider the resolution of parameters, such as strength excess, $\sigma^y - \sigma^o$, and slip-weakening distance, d_c, related to fault-constitutive properties, that may be obtained from the analysis of strong-ground motions. We show that waveform inversion of a synthetic strong-motion-data set from a hypothetical **M** 6.5 event resembling the 1979 Imperial Valley earthquake cannot uniquely resolve both strength excess and d_c. Specifically, we use a new inversion method to find two rupture models, model A having $d_c = 0.3\ m$ and high-strength excess, and model B having $d_c = 1\ m$ and low-strength excess. Both models have uniform initial stress and the same moment-rate function and rupture time distribution, and they produce essentially indistinguishable ground-motion waveforms in the 0–1.6 Hz frequency band.

These models are indistinguishable because there is a trade-off between strength excess and slip-weakening distance in controlling rupture velocity. However, fracture energy might be relatively stably estimated from waveform inversions. Our Models A and B had very similar fracture energies. If the stress drop is fixed by the slip distribution, the rupture velocity is controlled by fracture energy.

We show that estimates of slip-weakening distance inferred from kinematic inversion models of earthquakes are likely to be biased high due to the effects of spatial and temporal-smoothing constraints applied in such inverse-problem formulations.

Regions of high-strength excess are often used to slow or stop rupture in models of observed earthquakes, but our results indicate that regions of long d_c and lower

Guatteri and Spudich 2000

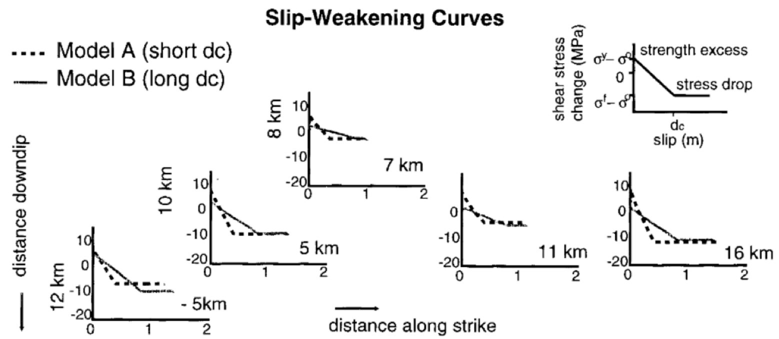

Figure 5. Slip-weakening curves at selected subfaults for model A (dashed line) and model B (continuous line) at different position along strike and different depths. We impose a fast weakening to model A (resulting in a slip-weakening distance of about 0.3 m) and a slow weakening to model B (resulting in a slip-weakening distance of about 1 m). Note that for model A the strength excess is systematically larger than that for model B.

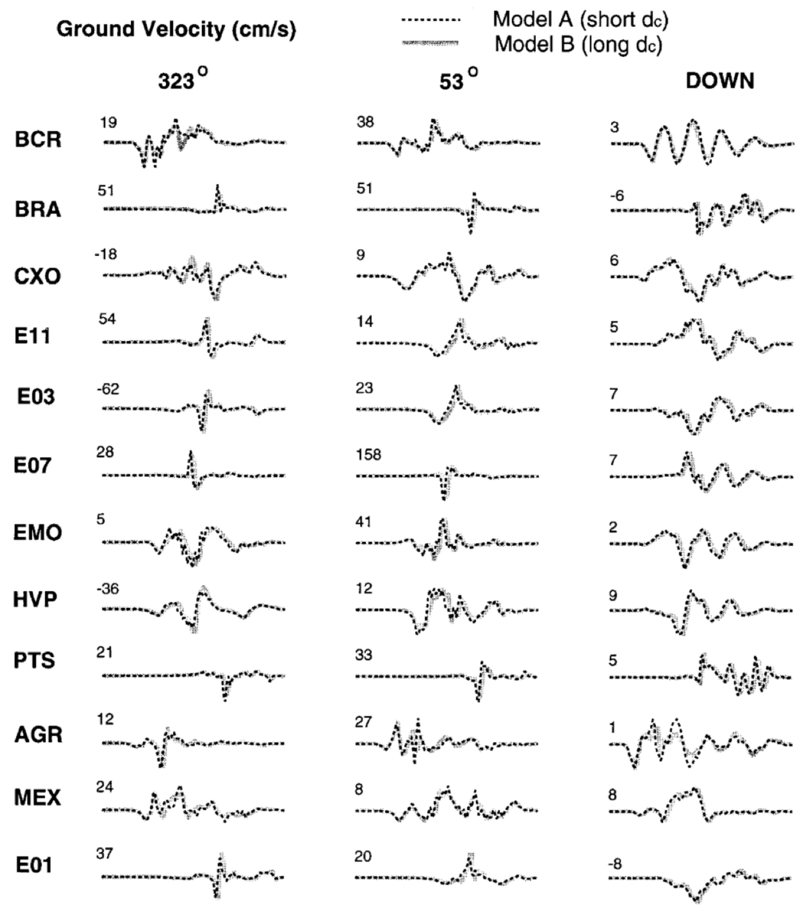

Main open questions

- How does shear stress (τ) vary with slip (δ) during earthquakes?
- What physical mechanism of weakening during slip? (different physical mechanisms can control dynamic weakening each of which has its own spatial and temporal length scales)
- Which are the dynamic parameters we are able to retrieve from seismological data?
- What fracture energy (G) is implied by the traction vs. slip relation? (seismological fracture energy is different from fracture energy in fracture mechanics)

Different attempts have been done to improve the knowledge of processes governing the constitutive behavior of faults

↓

Studies of the consistency of
Dynamic & Kinematic
Models

TRACTION EVOLUTION FROM KINEMATIC RUPTURE MODELS

An alternative approach to estimate the earthquake stress drop relies on computing stress parameters from traction evolution curves obtained from slip history at each point of the fault plane through pseudo-dynamic simulations.

Boundary condition: Slip velocity rupture history from kinematic inversions as a boundary condition on the fault plane.

Shear-stress histories are computed via the elastodynamic equations of motion

In literature, there are many papers that proposed the same procedure:
Bouchon 1997; Ide & Takeo 1997;Day et al. 1998; Dalguer et al. 2002; Fukuyama et al. 2003; Mikumo et al. 2003; Ripperger & Mai 2004;Tinti et al. 2005, Causse et al. 2014.

TRACTION EVOLUTION FROM KINEMATIC RUPTURE MODELS

Fukuyama and Madariaga 1998 derived the analytic relation among traction change on the fault plane and slip velocity:

direct term

$$T_\alpha(x_1, x_2, t) = -\frac{\mu}{2c_T}\dot{D}_\alpha(x_1, x_2, t) + \frac{\mu}{4\pi}\iint_{S+}\int_0^t K_{\alpha\beta\gamma}(x_1, x_2, t|\xi_1, \xi_2, \tau)\, \dot{D}_{\beta,\gamma}(\xi_1, \xi_2, \tau)\, d\tau\, d\xi_1\, d\xi_2, \quad (4)$$

Kernel of all points on the fault that are still slipping

where $K_{\alpha\beta\gamma}(x_1, x_2, t|\xi_1, \xi_2, \tau)$ is an integro-differential kernel. The derivatives $D_{\alpha,\beta}$ are the different components of Burger's vector, the distribution of dislocation density on the fault.

TRACTION EVOLUTION FROM KINEMATIC RUPTURE MODELS

Traction change

$$\sigma(x,t) = -\frac{\beta}{2\mu}\Delta\dot{u}(x,t) + \iiint \Delta\dot{u}(\xi,\tau)\mathrm{K}(x-\xi,t-\tau)\,d\xi\, d\tau$$

Fukuyama and Madariaga (1998)

By means of slip velocity history we can infer the traction change evolution on the fault plane. We solve the Elastodynamic equation using the rupture history as a boundary condition on the fault

Slip Velocity time history on the fault

$$\Delta\dot{u}(\xi,t) = \dot{f}(t - t_r(\xi))\cdot d(\xi)$$

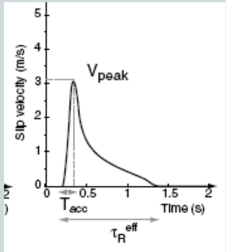

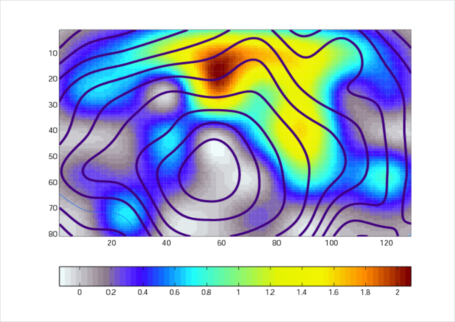

example: Slip distribution and rupture time from kinematic inversion

TRACTION EVOLUTION FROM KINEMATIC RUPTURE MODELS

Schematic sketch to compute traction change from kinematic rupture models.

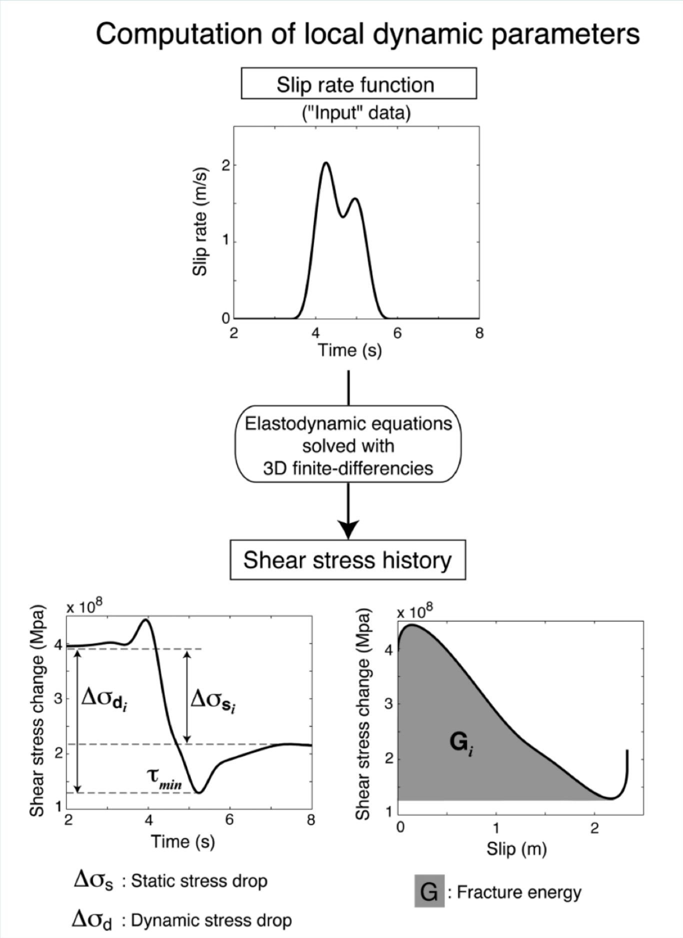

Causse et al 2014

Methodology

1. Traction at Split Nodes technique with 3D finite difference technique (Andrews 1999)

2. Boundary condition on the fault: prescibed slip velocity history (Ide and Takeo, 1997 and Day et al. 1998).

3. By solving the elastodynamic equation (Fukuyama and Madariaga 1998), we infer traction change evolution.

TRACTION EVOLUTION FROM KINEMATIC RUPTURE MODELS

Uniform model: slip=1m, Vr=2km/s, Tacc=0.225s

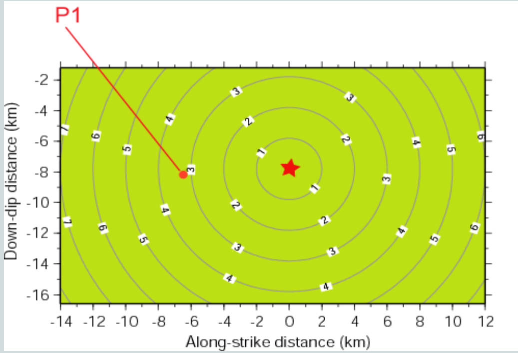

A common feature of dynamic models is that traction evolution within the cohesive zone shows a slip-weakening behavior, which in general may have a variable weakening rate (i.e., not linear).

The input is the prescribed rupture history in terms of slip velocity and rupture time

input

The peak stress is attained at nonzero slip and that a slip- hardening phase precedes the slip-weakening phase. This behavior is a consequence of imposing a bounded slip acceleration.

The traction evolution depends on the position on the fault because of different contributions of the dynamic load

output

output

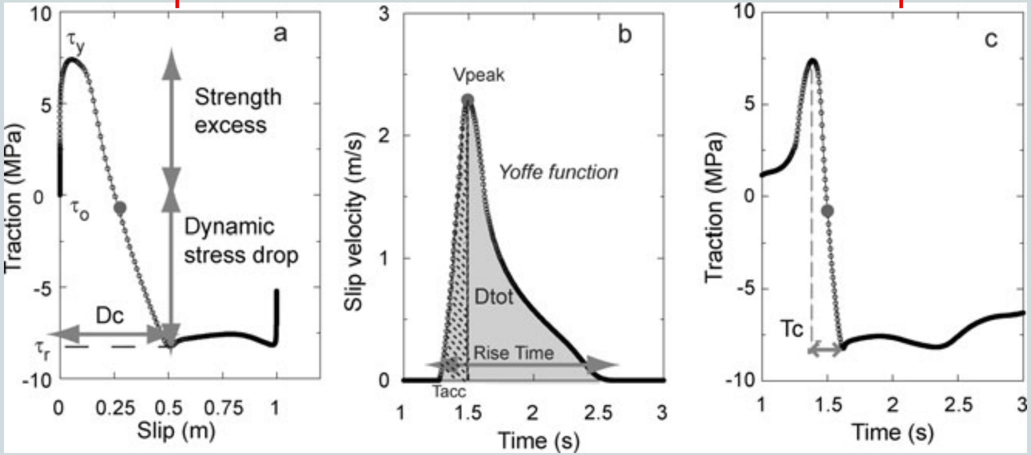

Example with a regularized Yoffe function

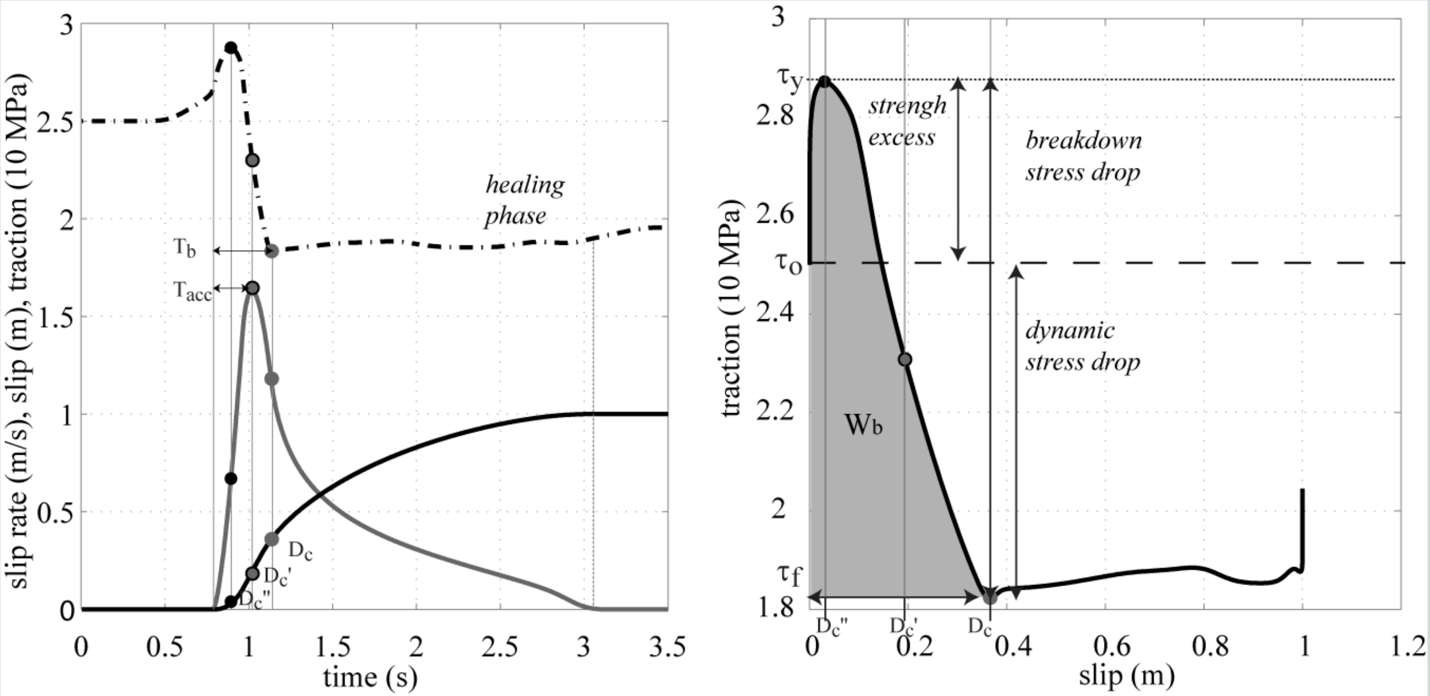

The breakdown phase occurs during the acceleration phase and the beginning of the deceleration.

TRACTION EVOLUTION FROM KINEMATIC RUPTURE MODELS

Important steps to compute traction evolution: Assumptions & limitations

1) Resolution is given by the kinematic model
2) Smoothing operator
3) Source time function resulting from the kinematic model
4) Initial Stress distribution

Resolution of the kinematic model

The dynamic computation require a finer grid than the kinematic models

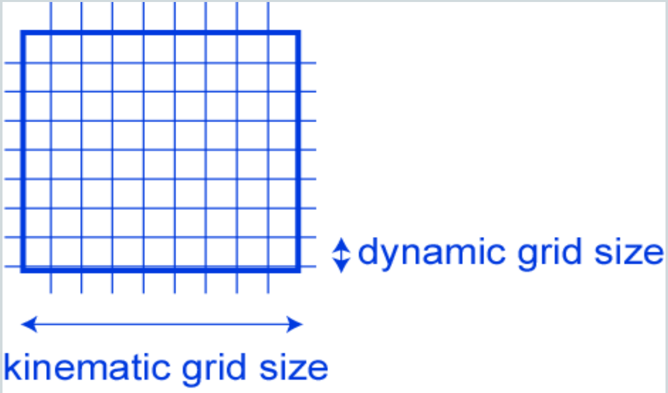

We used a spatial **BICUBIC INTERPOLATION**
(one of the smoothest technique to avoid the artificial singularity on the stress due to the gradient of slip distribution)

Resolution of the kinematic model

We preserve the SEISMIC MOMENT: not only the TOTAL MOMENT but the **LOCAL SEISMIC MOMENT** on each subfault of the kinematic model

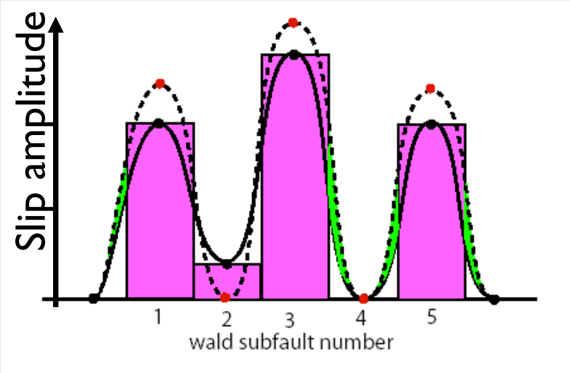

Black dots are the original kinematic values;
Red dots are the new points used for the spatial interpolation. In this way the well resolved (pink) areas are maintained.
We only overestimate the moment of the very small slip subfaults to avoid to introduce the negative values of slip.

Resolution of the kinematic model

1979 Imperial Valley
1994 Northridge

1992 Landers

Original slip model

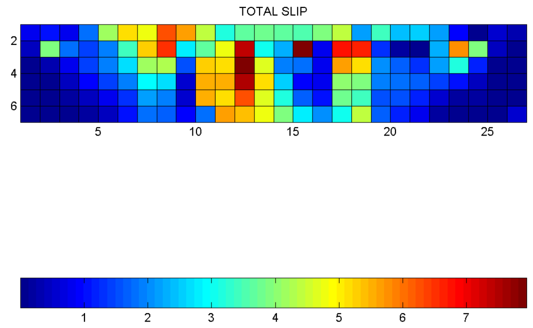

Interpolated slip model

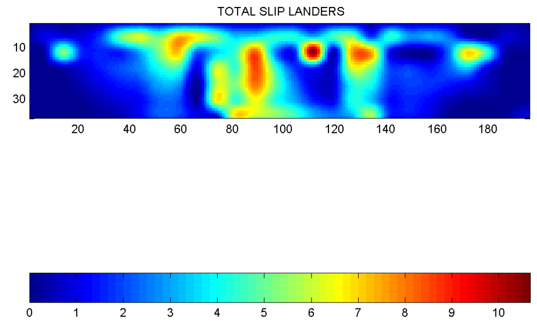

Smoothing operator

The dynamic calculations require a temporal smoothing with a running mean of slip velocity time history

1 Example: Northridge slip velocity evolution: 3 triangular functions overlapped

Without running mean **With running mean**

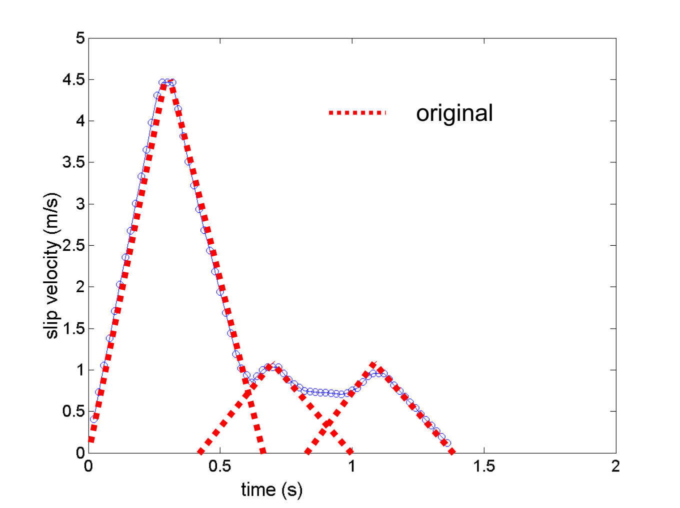

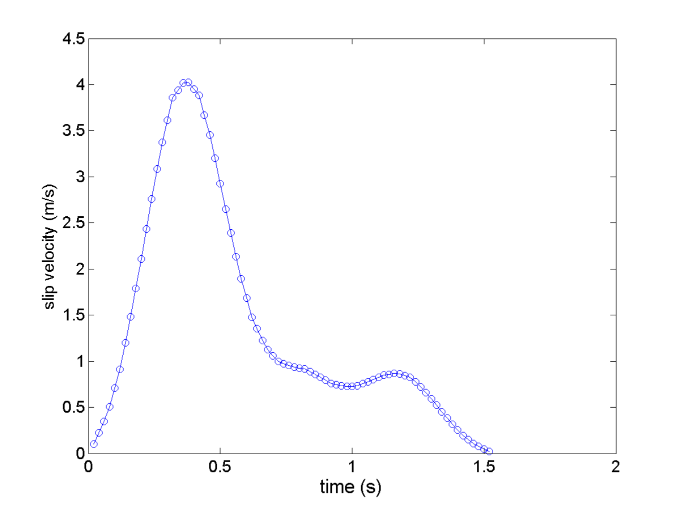

2 Example: Kostrov source time function, used in Morgan Hill kinematic model, has a singularity we eliminate through running mean

Smoothing operator

The dynamic calculations require a temporal smoothing with a running mean of slip velocity time history

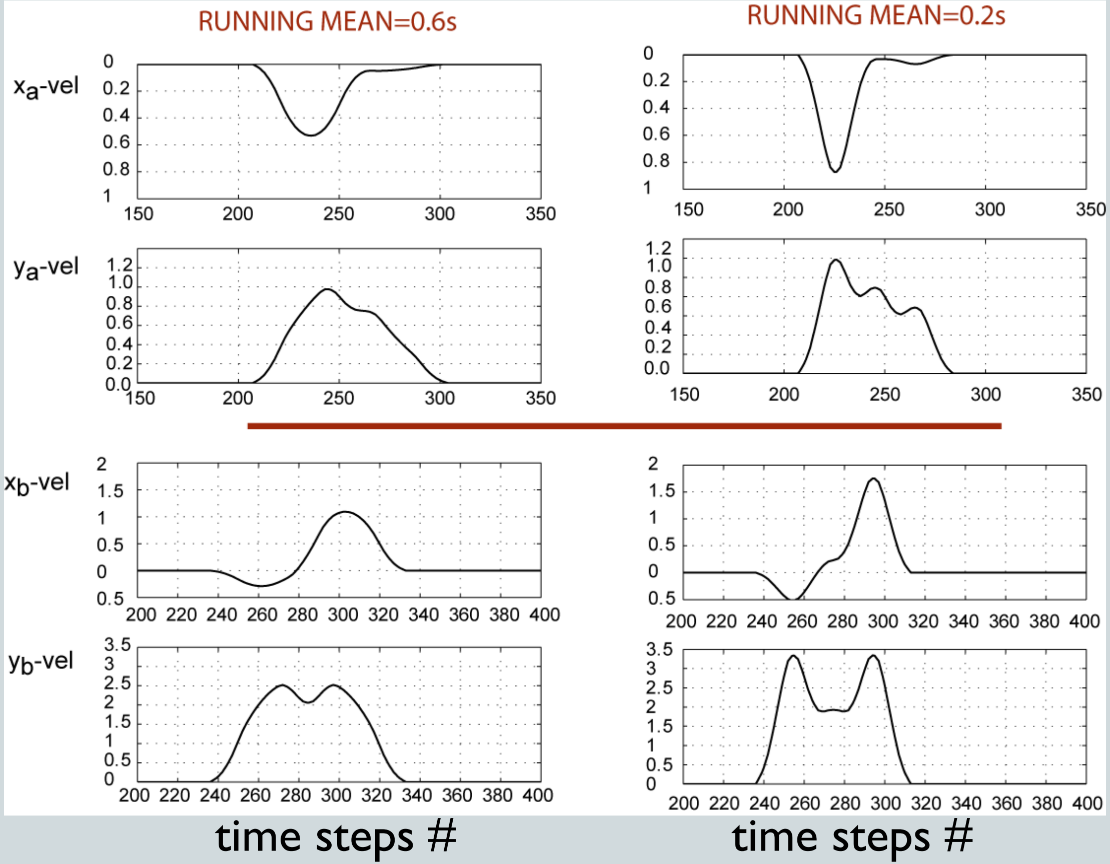

Initial Stress distribution

The seismic waves are only sensitive to the stress change (i.e. solution of dynamic computation is $\boxed{\Delta\vec{\tau}(\vec{x},t)}$

Total traction is: $\boxed{\vec{\tau} = \vec{\tau}_0 + \Delta\vec{\tau}}$

The initial stress vector is unknown

Assumptions on the initial stress are required to interpret the traction evolution and to compute the traction versus slip curves and the dynamic parameters on the fault. This is particularly important if traction is not necessarily collinear with slip velocity.

We have to specify the magnitude and direction of INITIAL STRESS.

Initial Stress distribution

The slip history taken from kinematic models allows the spatial and temporal variations of slip direction.

Spatial heterogeneous rake

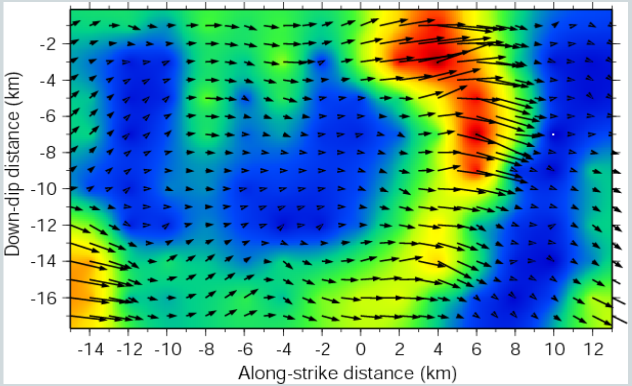

Slip distribution on the fault

Temporal heterogeneous rake

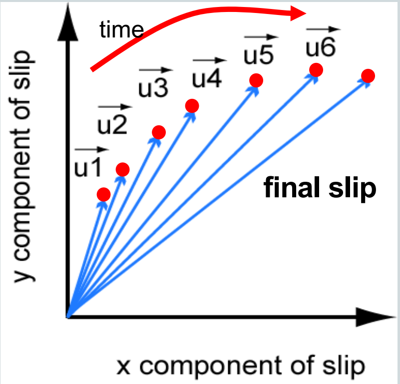

Temporal evolution of slip for a target point

Initial Stress distribution

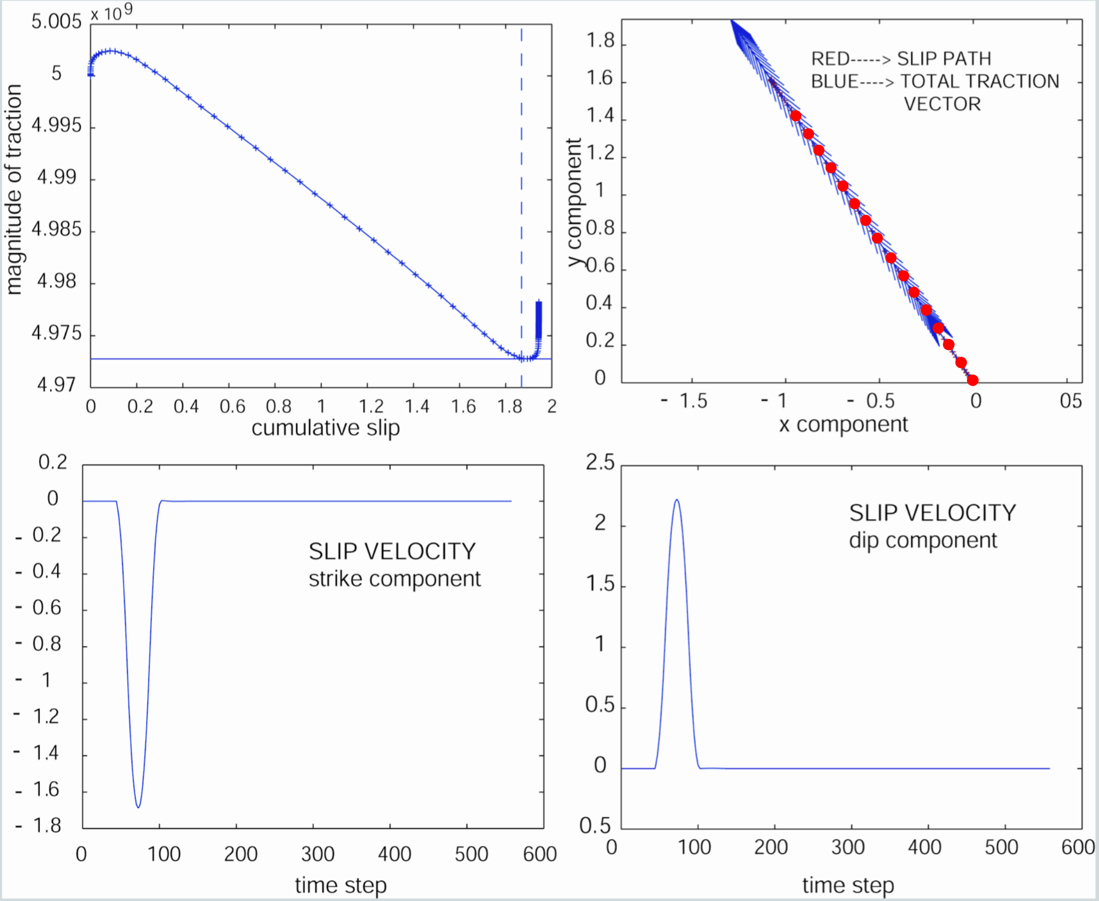

Initial Stress distribution

Constitutive behavior & Slip Velocity

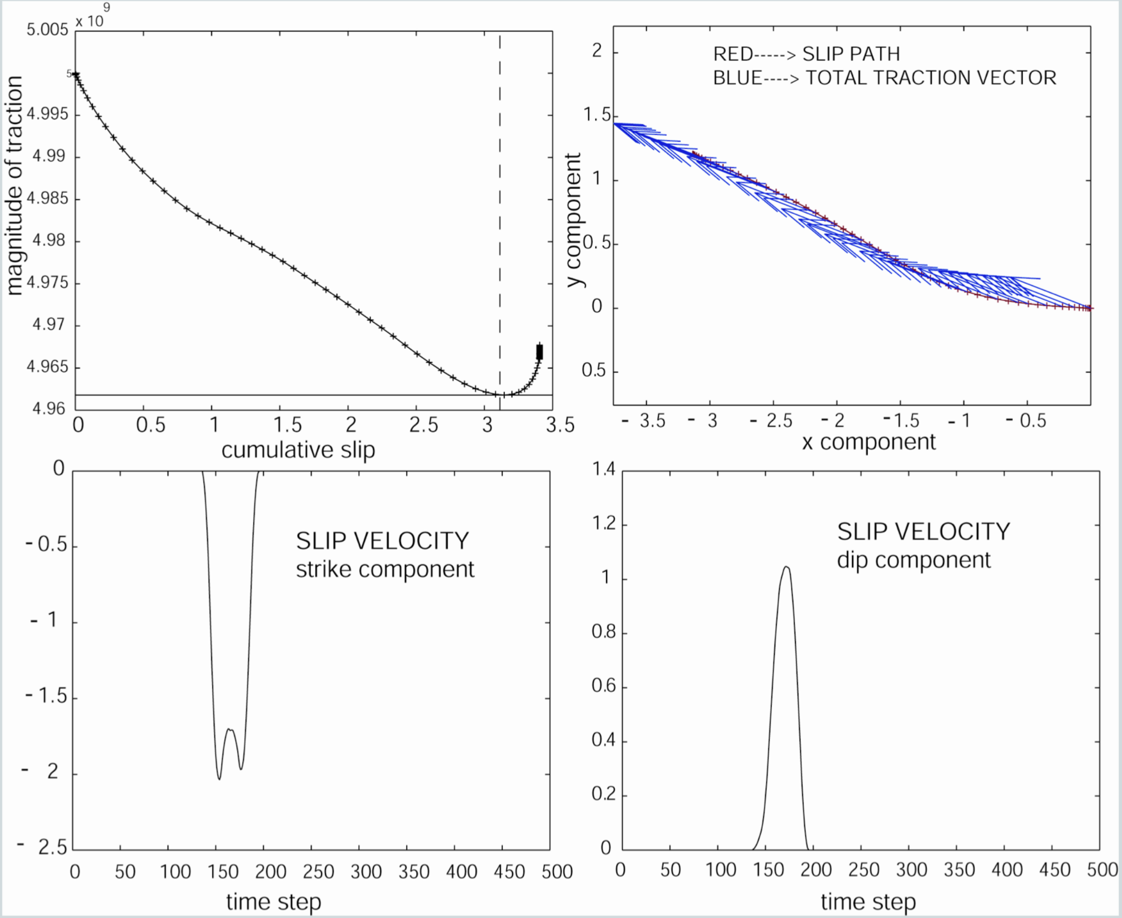

Initial Stress distribution

Constitutive behavior & Slip direction

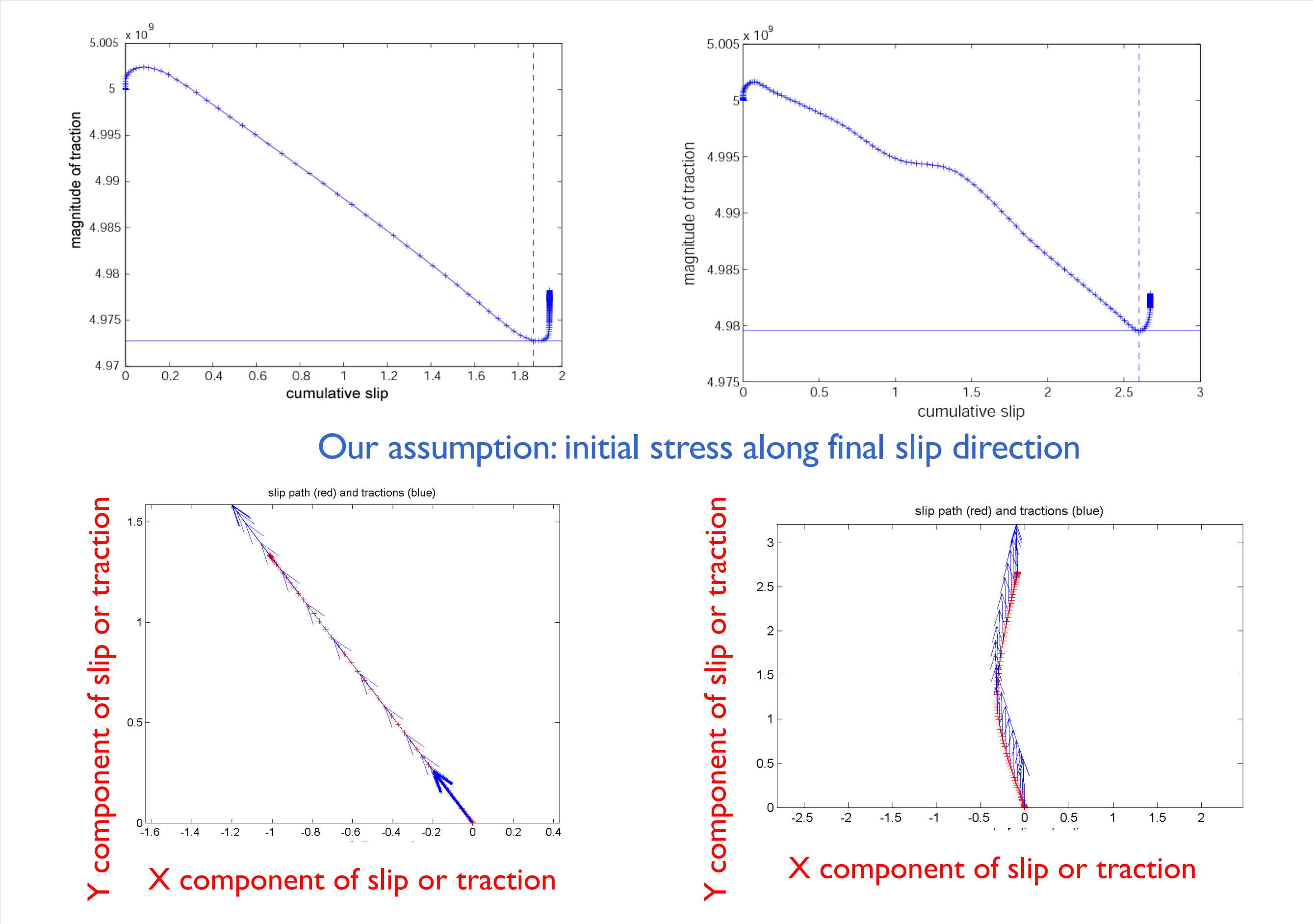

Initial Stress distribution

The choice of initial traction (direction & amplitude) controls the collinearity condition between total stress and slip velocity.

OUR ASSUMPTION:
Initial traction is aligned with the local direction of the final slip

- Among different choices it is physically consistent
- Total traction can have heterogeneous direction on the fault plane
- If there is a temporal rake rotation the collinearity is not guaranteed for all the time step

Example of retrieved traction change evolution

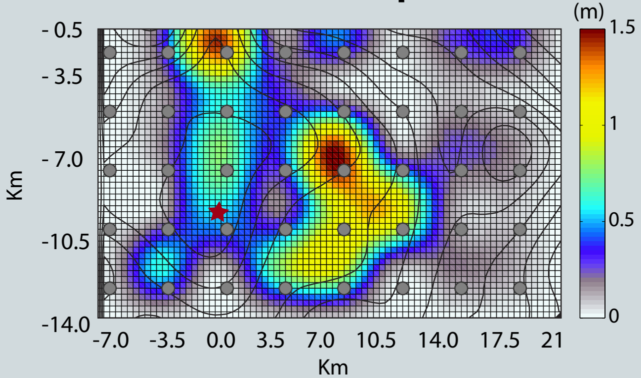

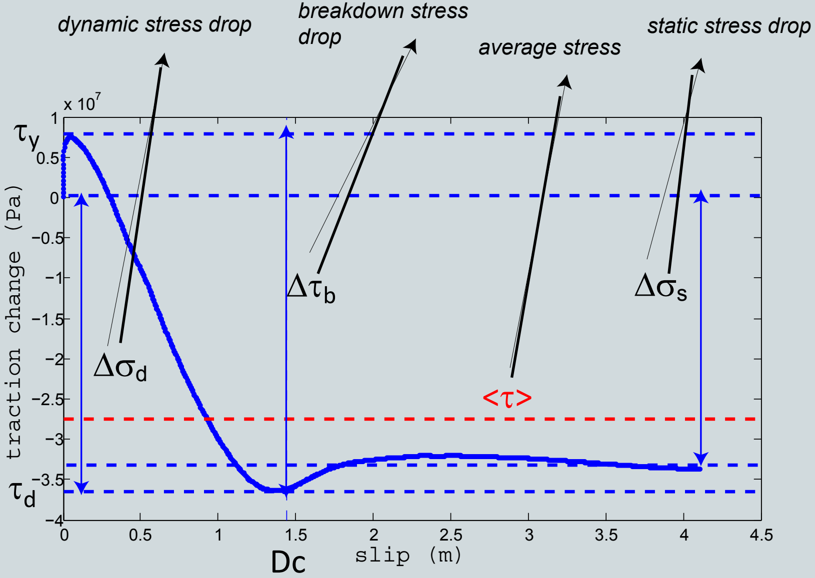

2009 L'Aquila earthquake Mw=6.1

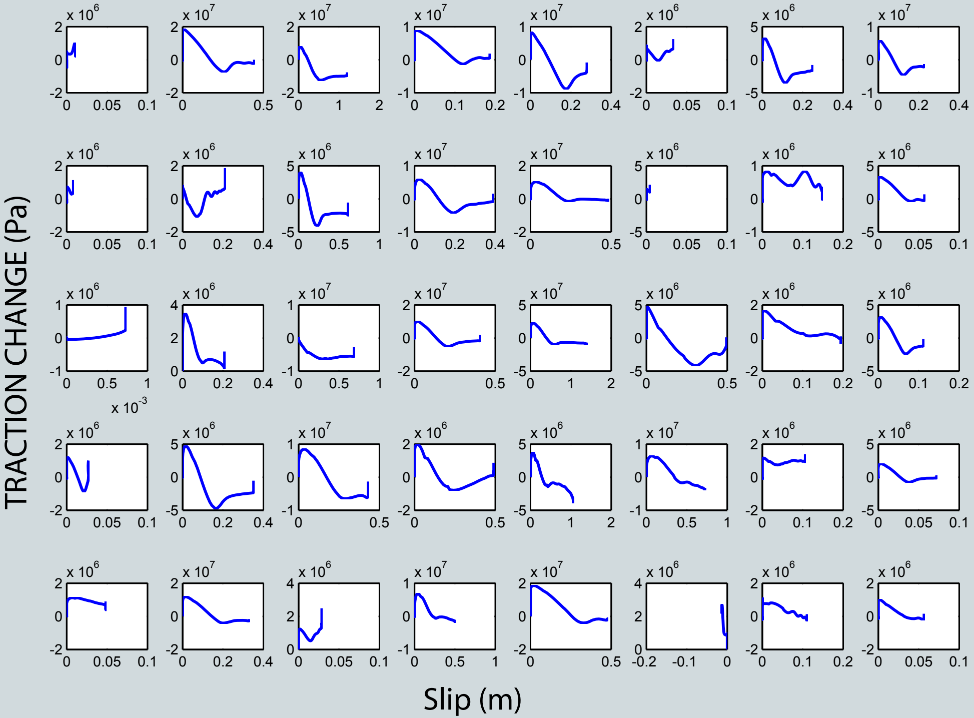

Example of retrieved traction change evolution

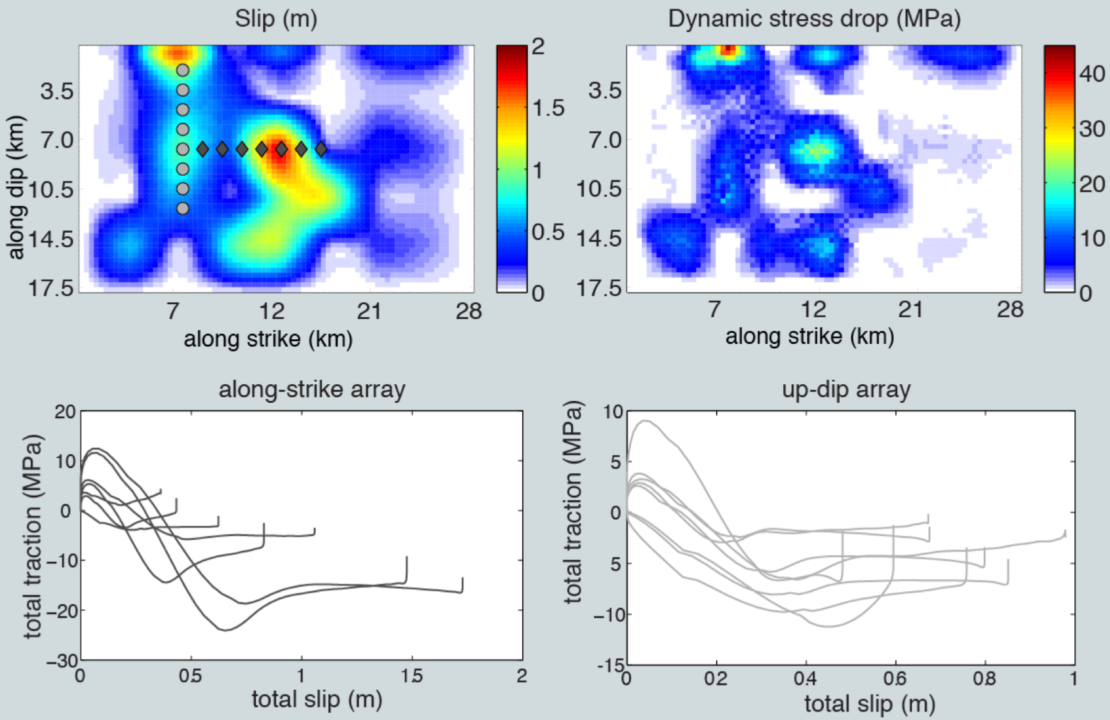

2009 L'Aquila earthquake Mw=6.1

Fracture energy

The fracture energy is one of the key ingredients required to describe the energy flux per unit area at the crack-tip.

Fracture energy (G) is commonly associated with the area below the shear traction curve and above a residual stress level <u>which is independent of slip.</u>

$$G = G(\delta) = \int_0^{D_c} \left[\tau(\delta') - \tau_{res} \right] d\delta'$$

This fracture energy is considered a measure of the load sustaining fracture propagation.

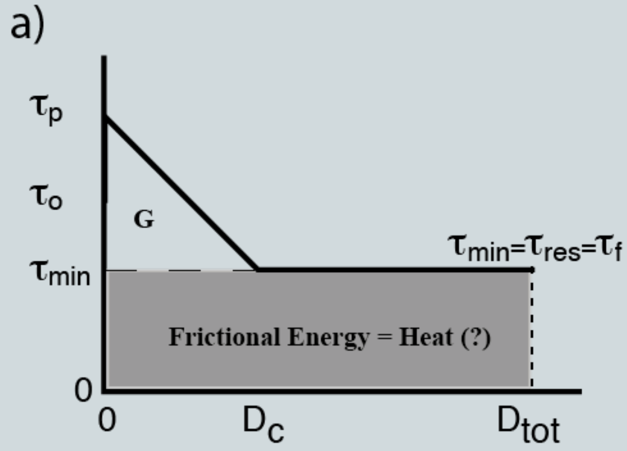

Fracture energy

$$G = G(\delta) = \int_0^{D_c} \left[\tau(\delta') - \tau_{res}\right] d\delta'$$

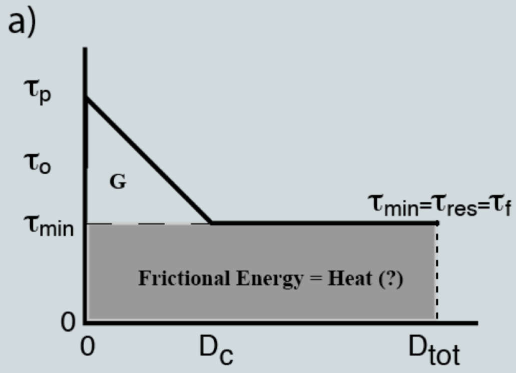

However, this definition is ambiguous when applied to traction vs. slip curves derived from kinematic slip models in which both traction and slip are non-collinear vectors and when traction does not decay to a constant level.

Depending on the assumptions in the kinematic models, the slip-stress relations can show either a linear weakening phase or extremely variable weakening behavior and sometimes, in subfaults with small slip, only a strengthening behavior.

Fracture energy

This plot illustrates a more general formulation in which the strength-hardening phase has a finite duration and a not negligible slip (Da), the stress degradation for increasing slip during the breakdown phase is not characterized by a linear decay and the residual stress depends on slip.

This behavior can generate slip velocity pulses.

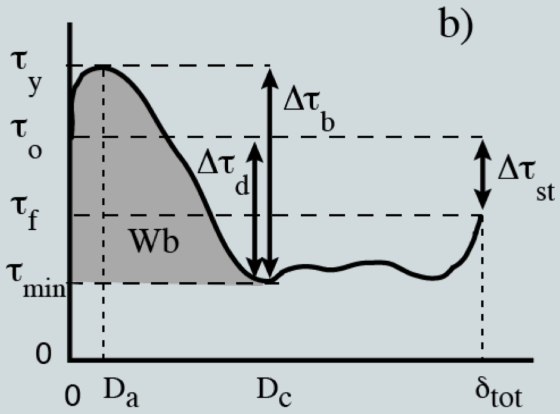

Breakdown work or Seismological Fracture energy

In more general cohesive or dissipative models, fracture energy represents an estimate of the mechanical work absorbed on the fault plane during rupture.

Breakdown work or seismological fracture energy is taken to be the excess of work over the minimum magnitude τ_{min} of traction during slip. We compute breakdown work (Wb) as the integral of the traction versus slip curve from zero slip to the point where the traction drops to τ_{min} .

$$W_b = \int_0^{T_b} (\vec{\tau}(t) - \vec{\tau}_{\min}) \cdot \vec{v}(t) dt$$

$$W_r = \int_{T_b}^{T} (\vec{\tau}(t) - \vec{\tau}_{\min}) \cdot \vec{v}(t) dt$$

This measure is applicable when rake rotates with time and when there is no constant residual stress. Dot product among two vectors.

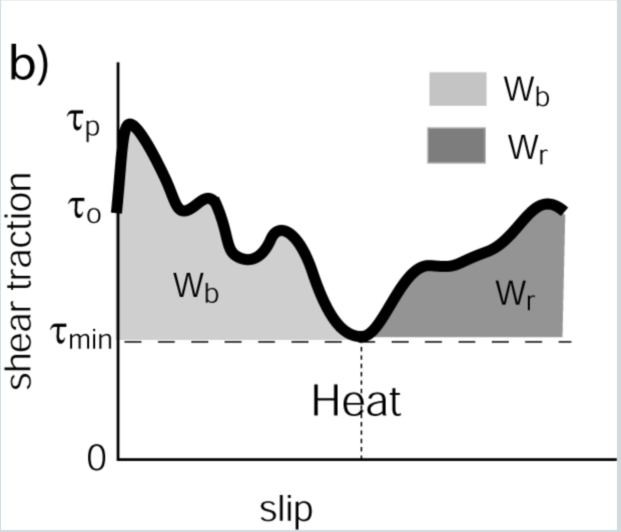

The breakdown work is a measurable quantity characterizing the mechanical work absorbed on the fault.

Breakdown work or Seismological Fracture energy

The gray area is the energy density. For real earthquakes, it might contain an mixture of heat and surface energy. The boundary between heat and surface energy (energy that goes into fracture and gouge formation) probably does not lie along a horizontal line at τ_{min}. This means that the breakdown work may be expended in both heat and gouge formation/evolution during dynamic slip episodes.

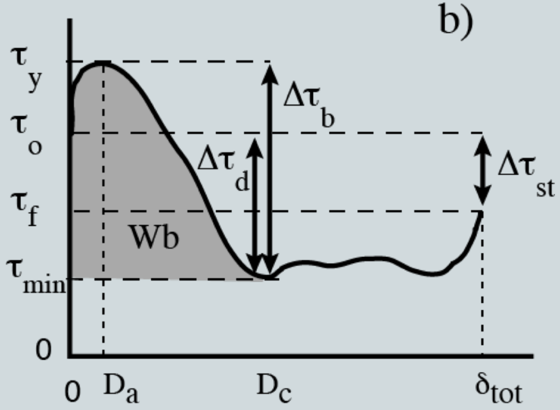

Breakdown work is a · a 'phenomenological' parameter and characterizes several processes occurring at the expanding crack tip such as micro cracking, off-fault plasticity, energy loss due to heat and other energy dissipative phenomena.

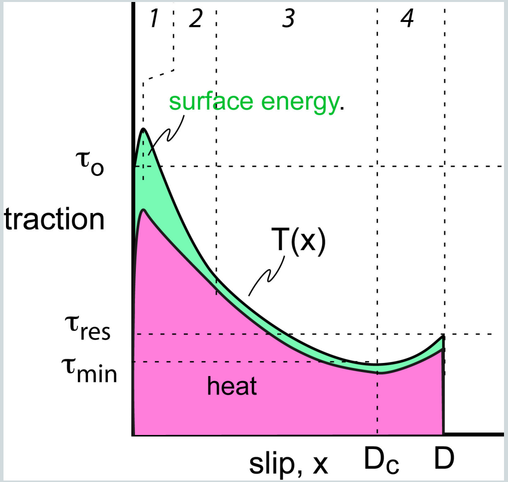

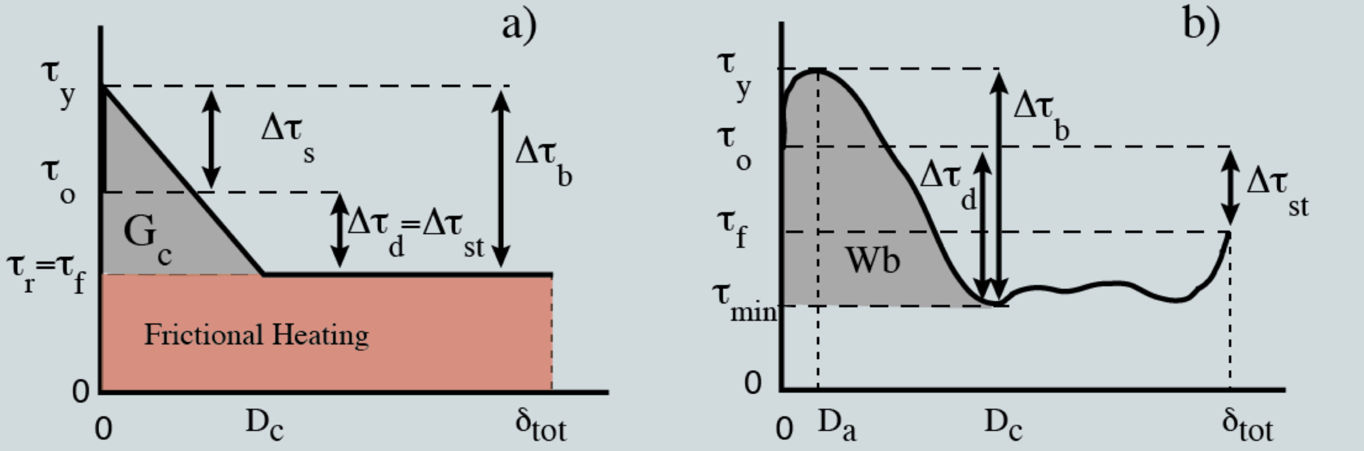

For real earthquake it might be misleading to call this quantity "fracture energy." This term has different meanings in different contexts. In fracture mechanics, fracture energy is the energy consumed at the crack tip to create a surface without incurring any slip.
In the Slip-Weakening models, the area was called the fracture energy because it played the same role as fracture energy in fracture mechanics, absorbing energy near the crack tip and controlling rupture speed.

Breakdown work represents the only measurable portion of the mechanical work dissipated within the fault zone, since the absolute stress level on the fault is unknown.

2009 L'Aquila event

These simulations suggest that, if the slip velocity function would be known, the slip-weakening distance Dc could be measured from slip-weakening curves retrieved from rupture history.

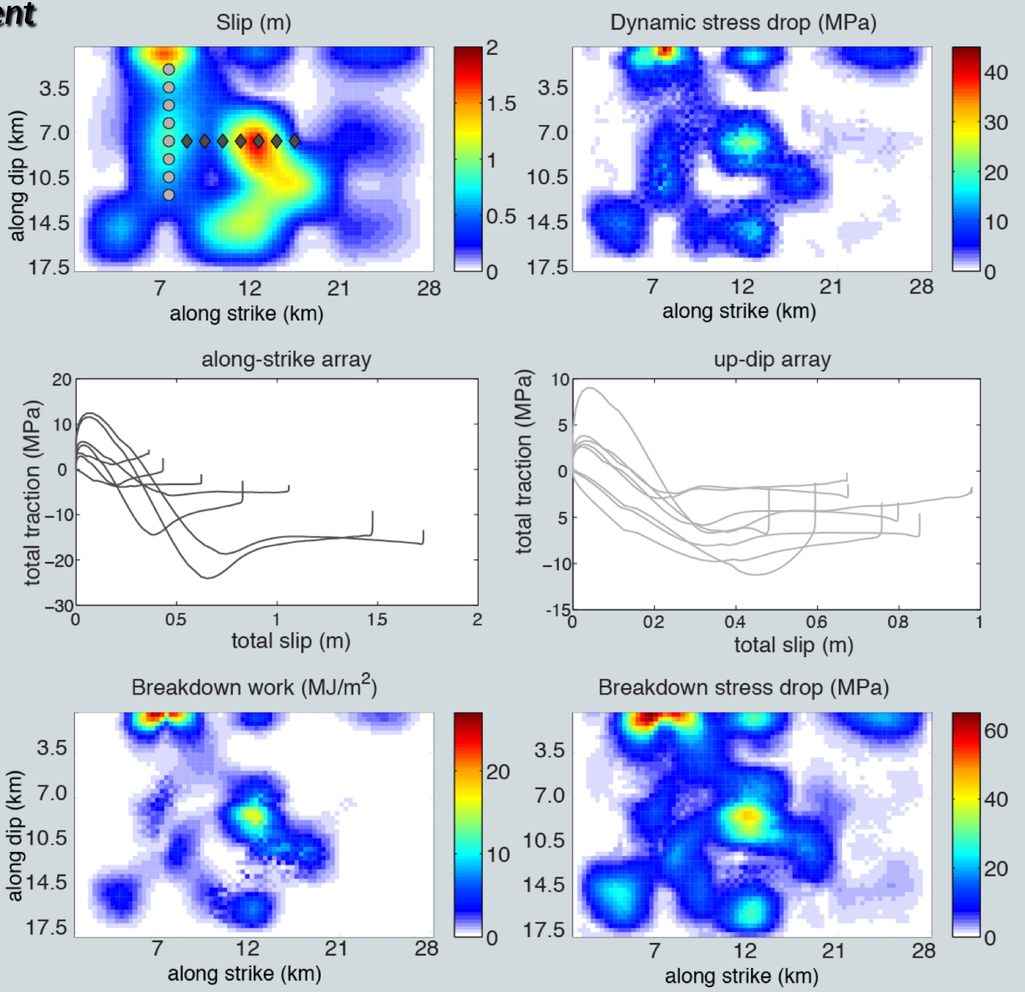

(seismological fracture energy)

1994 Northridge

Total slip

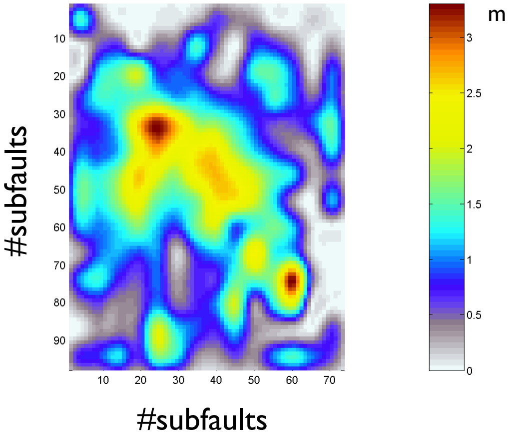

Dc

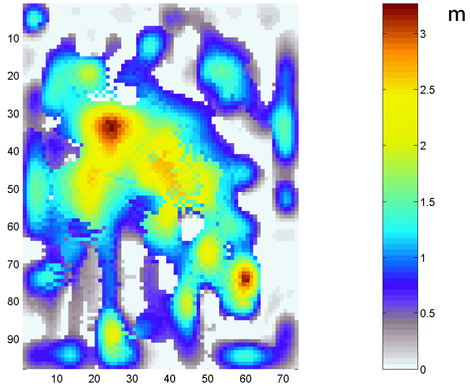

Fracture Energy

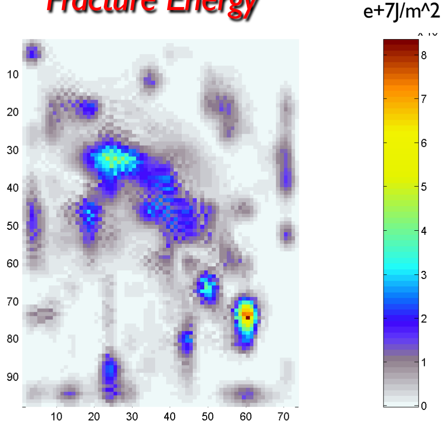

Kinematic model: Wald et al. 1998
Fault dimension: 18 Km x 24 Km
Source time function: 3 triangular windows
Average rake is 101°
Grid size: dx=0.25km #subfaults: 7081

1992 Landers

TotalSlip

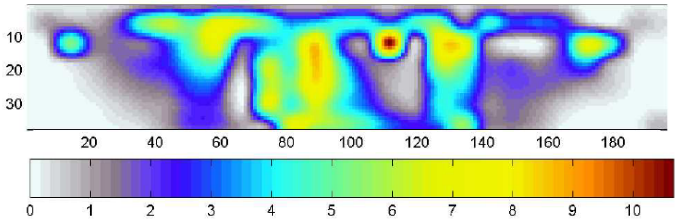

Fracture energy

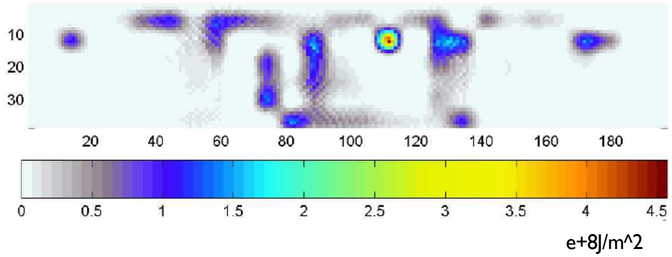

Stress drop

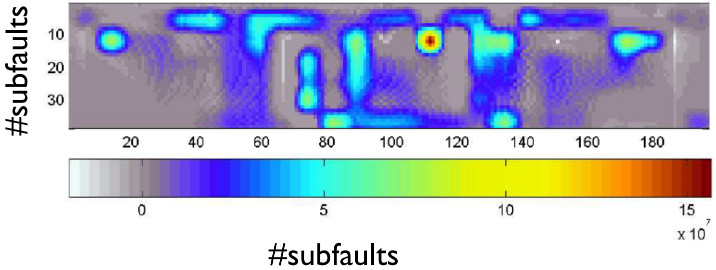

Kinematic model: Wald and Heaton 1994

Fault dimension: 78 Km x 15 Km *Camp Rock-Emerson (length 36km)+ Homestead Valley (length 27km) + Landers-Johnson Valley (length 30km)*

Source time function: 6 triangular window

Rake is 0°

Grid size: dx=0.4km ;#subfaults:7448

Questions:

1. Effect of slip velocity on the retrieved estimates of Dc?

2. Relation among kinematic and dynamic parameters?

3. Resolution of dynamic parameters?

4. Which is the scaling law (in terms of fracture energy and stress drop) we can infer from these models?

5. What about average values of these quantities?

Example: uniform model

Inferred dynamic traction evolutions for 4 different source time functions: smoothed ramp function, an exponential function and two regularized Yoffe functions.

The dynamic modeling is very sensitive to the adopted source time functions.

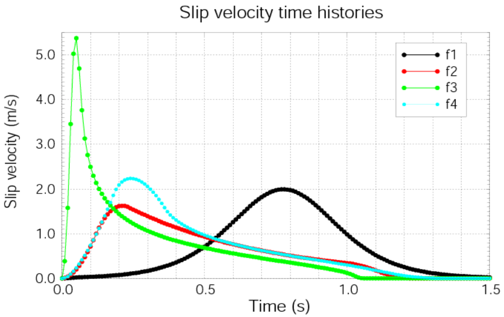

Slip = 1 m

Rise time = 1 s

Rupture velocity = 2 km/s

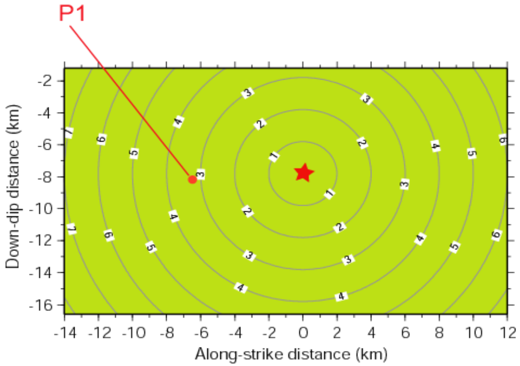

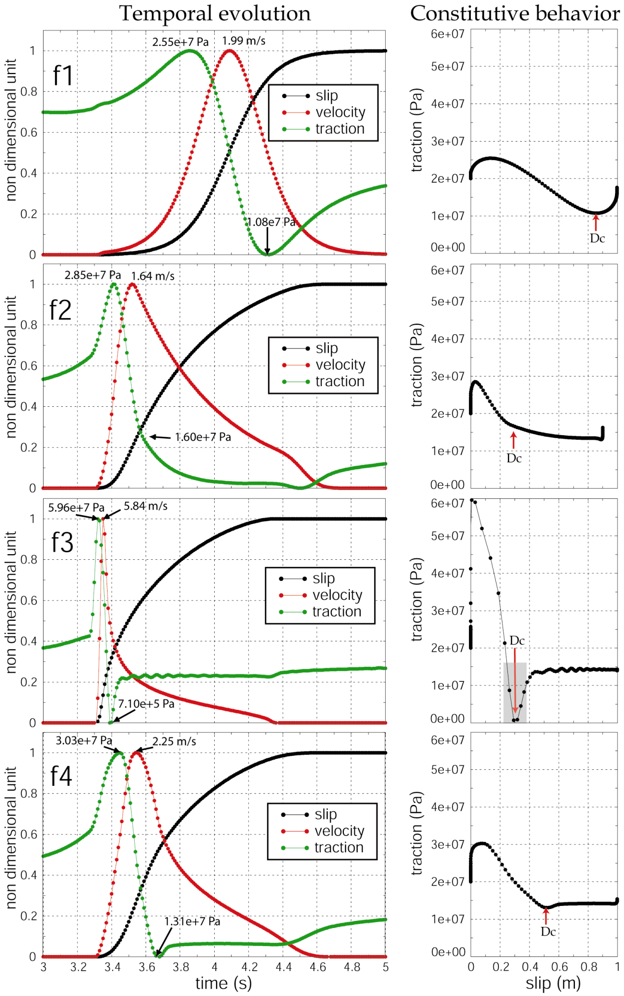

Effect of slip velocity on the retrieved estimates of Dc

3D Uniform source model

Forward waveform modeling

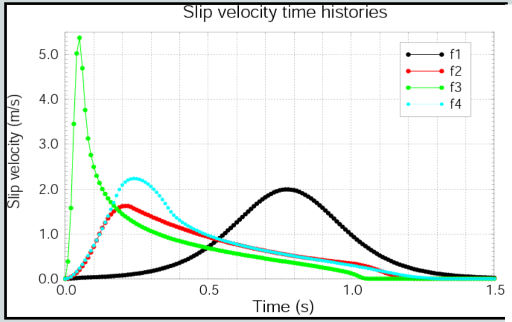

Station 2
Epicentral distance 37 km

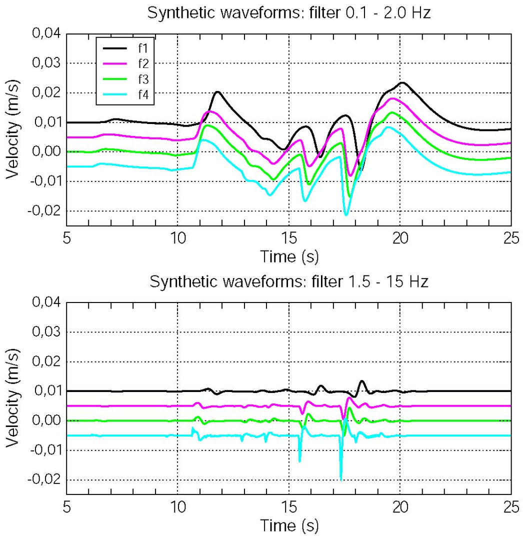

Station 1
Epicentral distance 13 km

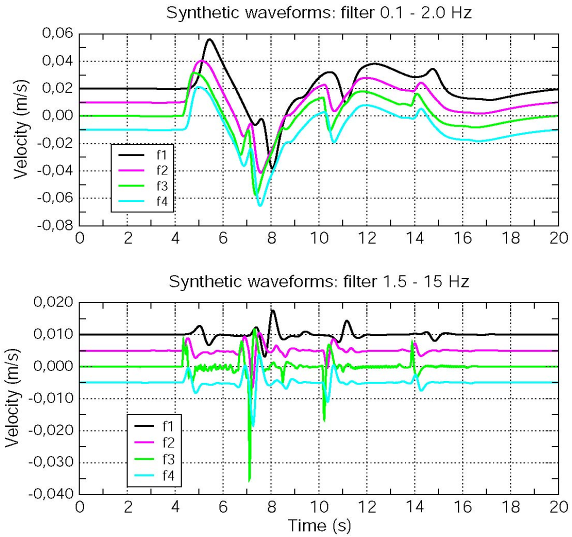

Effect of slip velocity on the retrieved estimates of Dc

Example: heterogeneous Slip distribution and Rupture Time

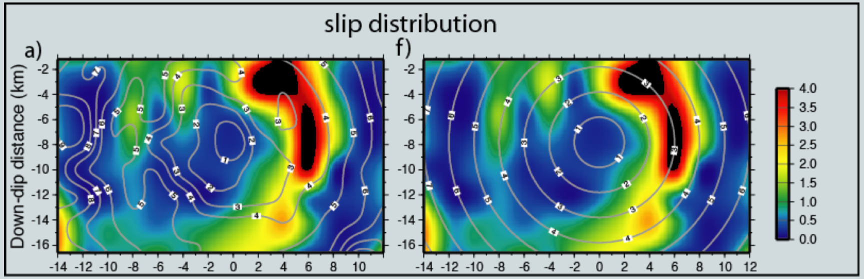

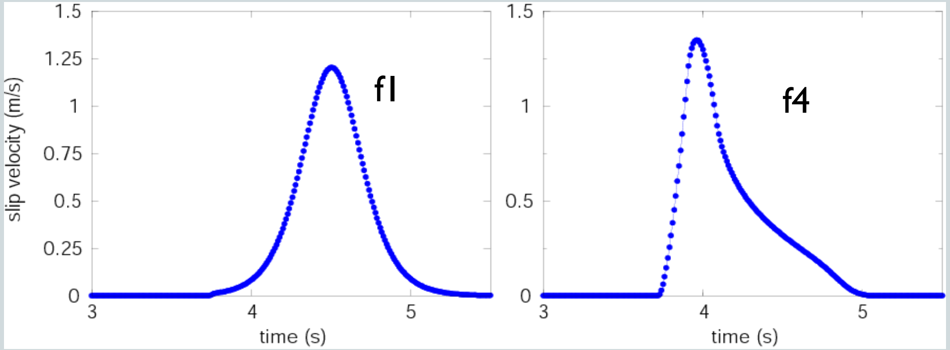

We compare the dynamic models inferred by using the same slip distribution and rupture time but two different source time functions

Effect of slip velocity on the retrieved estimates of Dc

Strength excess and Dynamic stress drop distribution

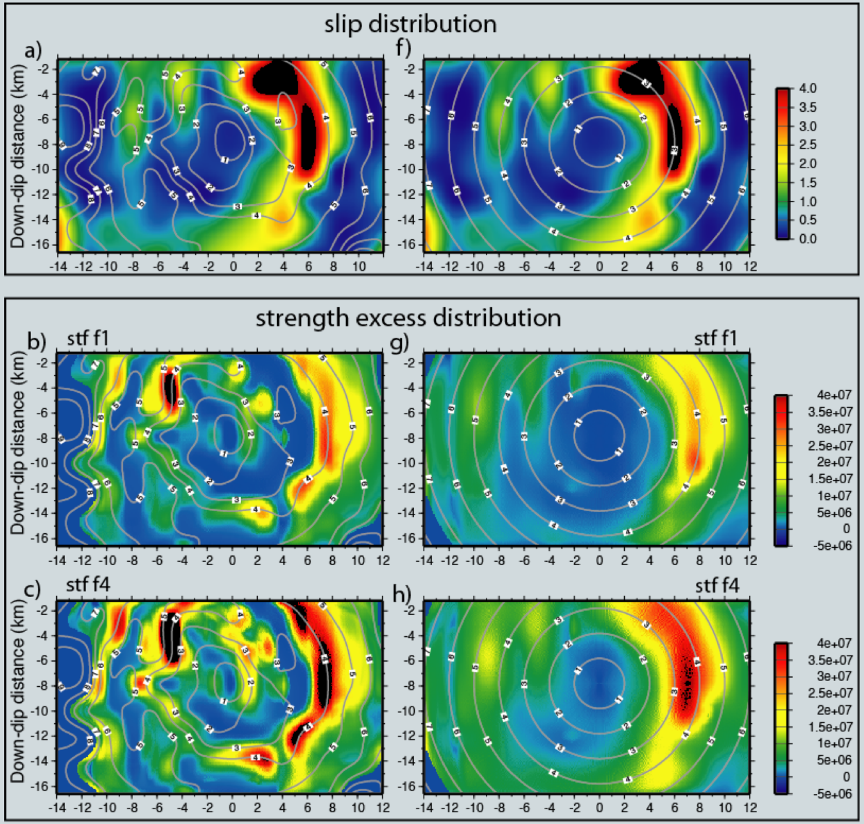

For the model with variable rupture time, high values of strength excess are found in correspondence of zones where the crack tip decelerates; for model with constant rupture time the strength excess mainly depends on peak slip velocity.

Source time function f4 produces larger strength excess amplitudes than those calculated from f1, due to the fact that f4 has a steeper initial slope and generates larger slip accelerations than f1.

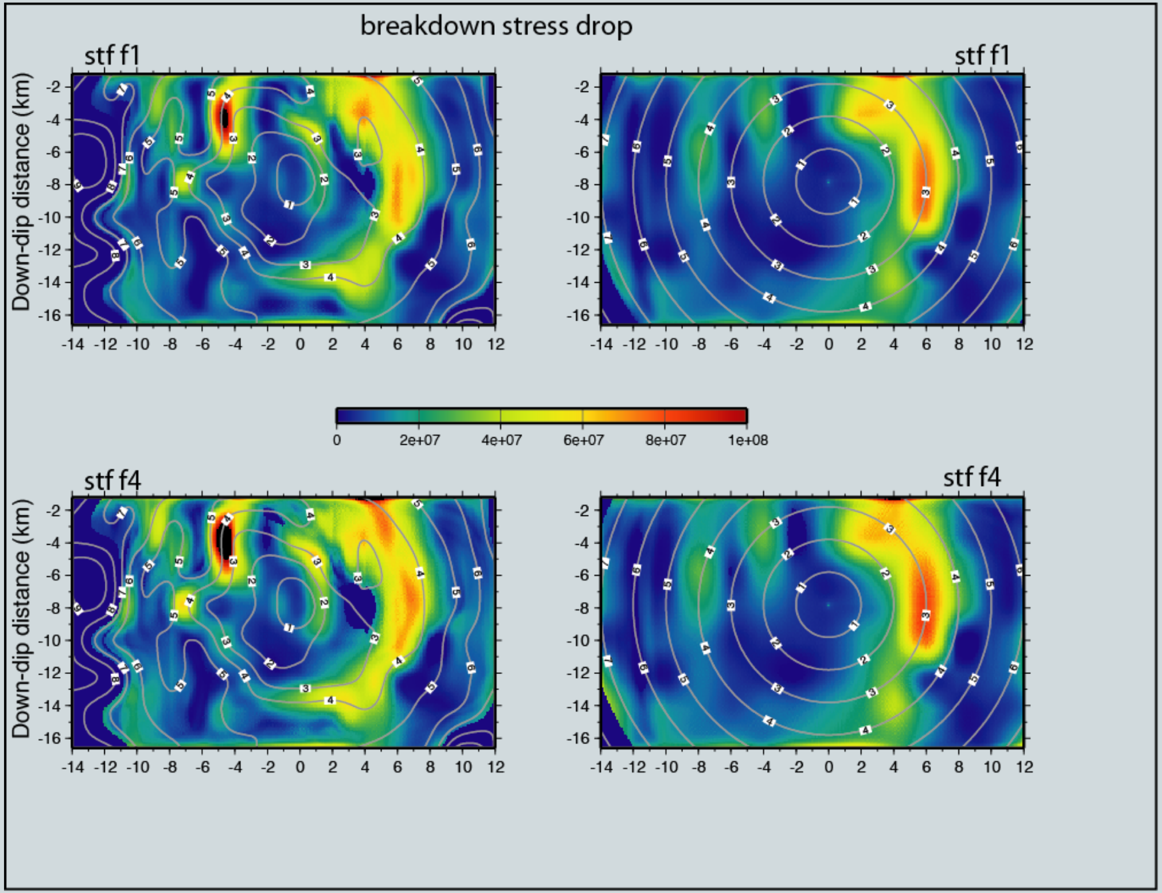

Breakdown stress drop is defined as the difference between the yield and the frictional stress. This figure illustrates that the breakdown stress drop is less dependent on the adopted source time function than strength excess or dynamic stress drop.

Effect of slip velocity on the retrieved estimates of Dc

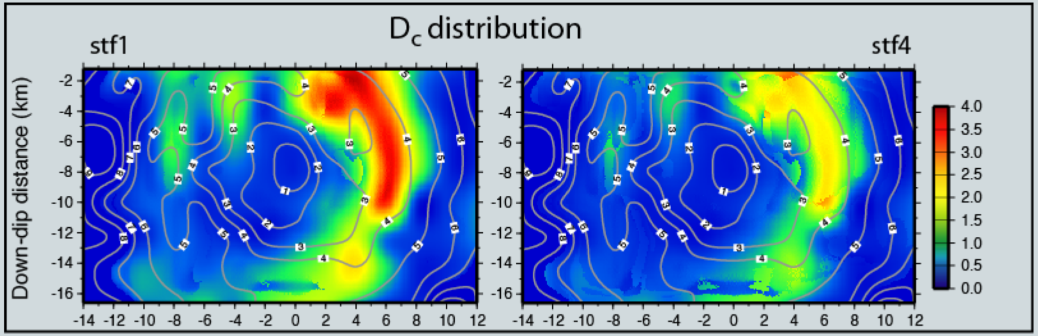

Dc is 80% of total slip with f1 and 50% of total slip with f4.

The spatial distribution of Dc inferred for both f1 and f4 is correlated with the final slip distribution.

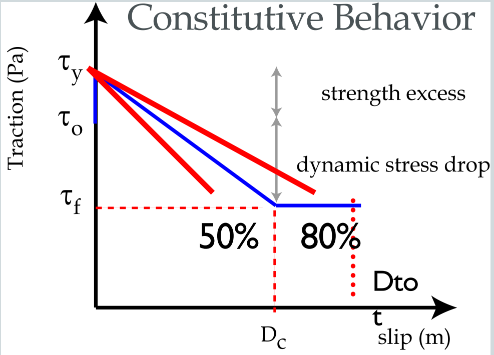

The ratio between Dc and final slip value is nearly constant and controlled by the adopted source time function.

Dc is 80% of total slip with f1 and 50% of total slip with f4. In both cases Dc is strongly correlated to the final slip.

Can we believe to these results?
The physical interpretation of Dc should be done with caution.
The obtained dynamic parameters might be biased especially when STF is not compatible with elastodynamics are used.

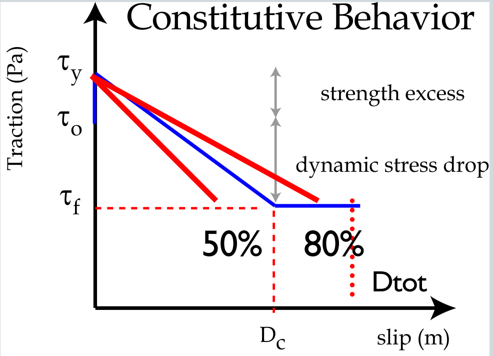

Relation among kinematic and dynamic parameters

This figure illustrates the effects of the assumed Yoffe function on several stress parameters. Left panels illustrate the effects of acceleration time (Tacc), while right panels show the effects of slip duration.

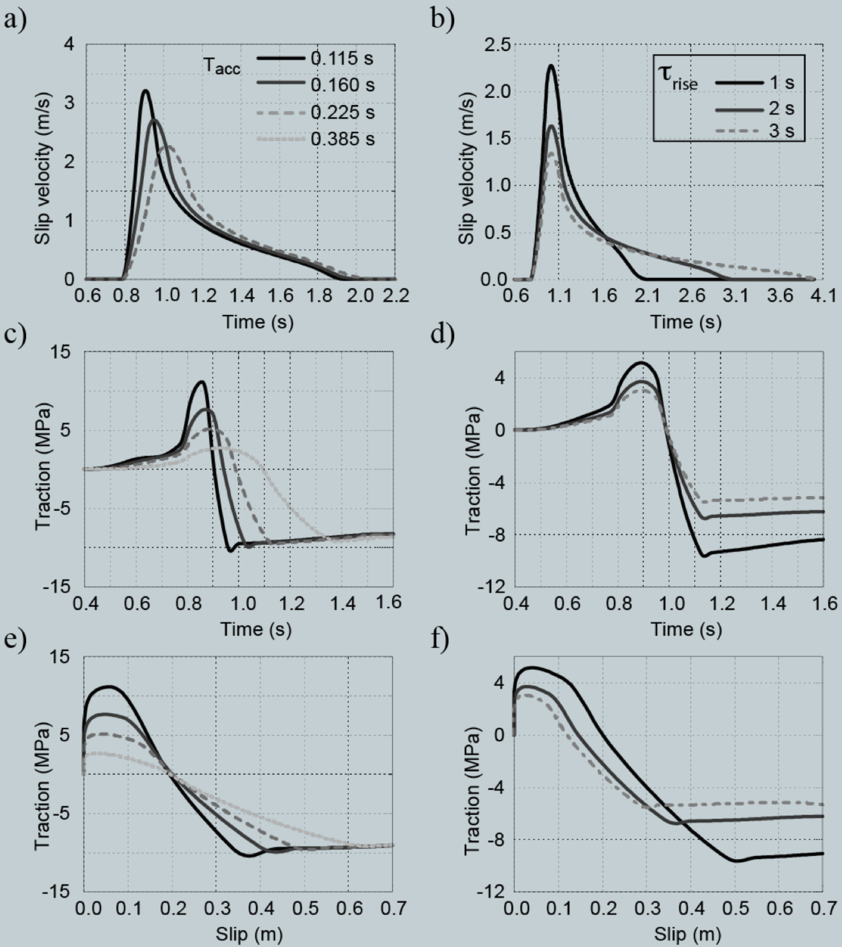

Relation among kinematic and dynamic parameters

Varying Tacc

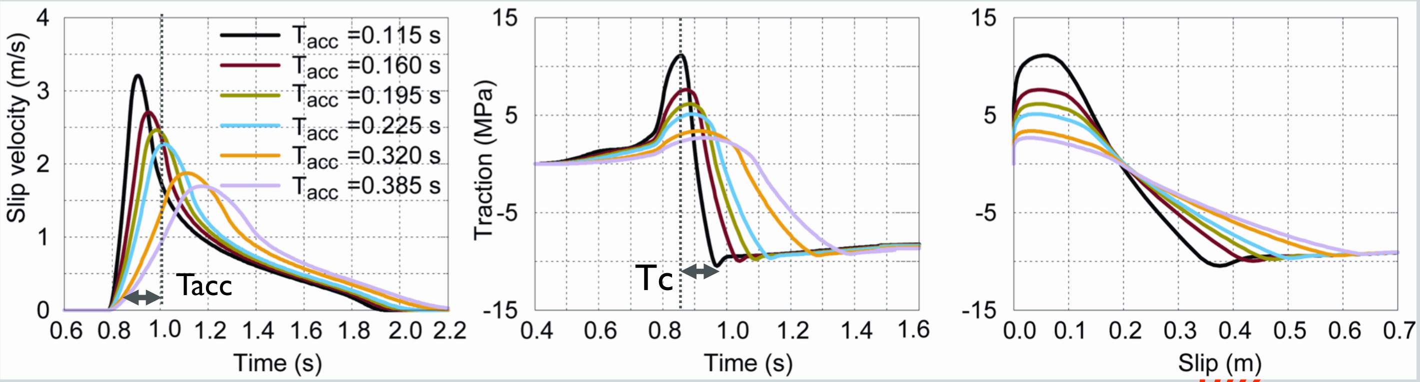

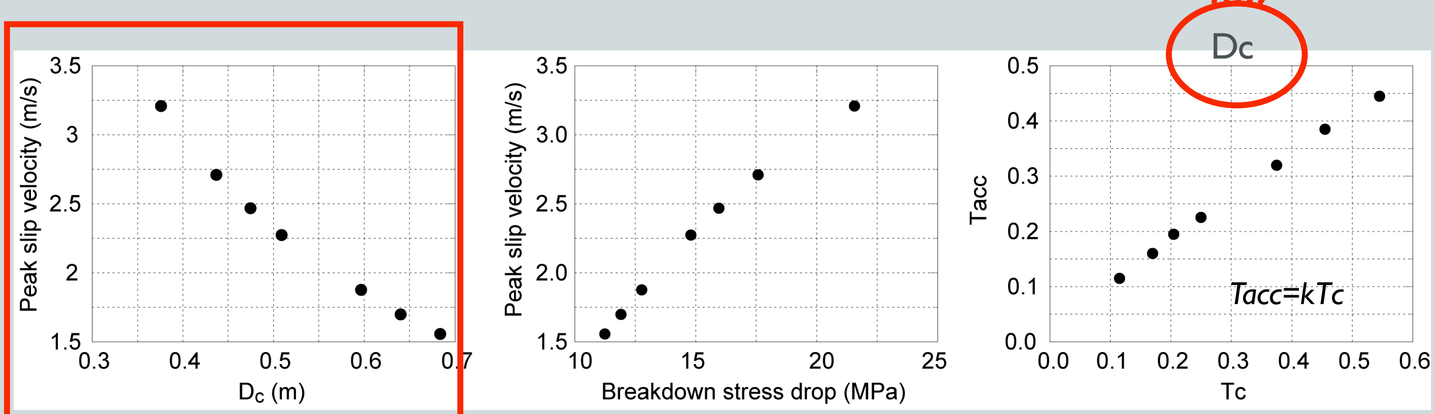

$$V_{peak} \propto \frac{D^2{}_{max}}{D_c \tau_R}$$

The Tacc is linearly related to the breakdown time

Relation among kinematic and dynamic parameters

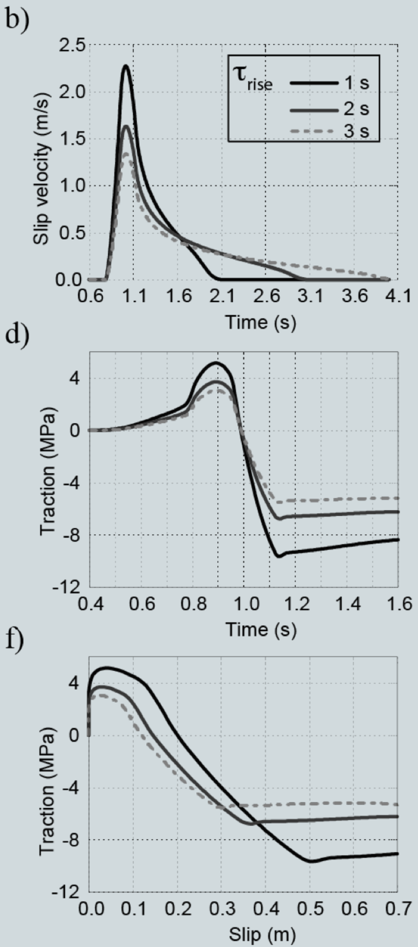

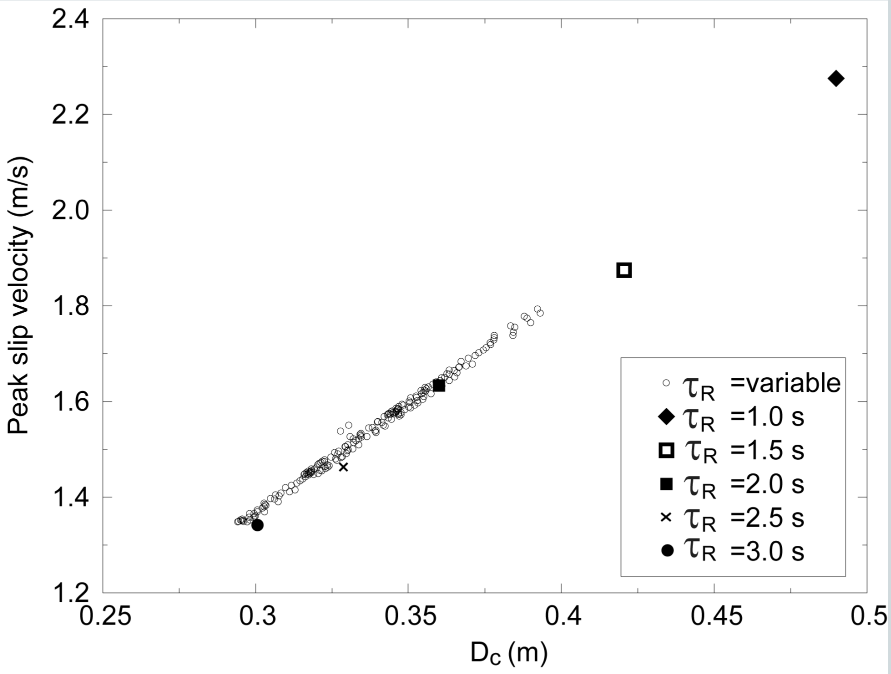

Varying rise time & peak slip velocity

$$V_{peak} \propto \frac{D_c}{T_{acc}}$$

For constant Tacc

Empirical Dynamic Relation for uniform kinematic model

Constant T_{acc} $$V_{peak} \propto \frac{D_c}{T_{acc}}$$

Constant τ_R $$V_{peak} \propto \frac{D^2_{\max}}{D_c \tau_R}$$

$$\boxed{D_c \propto \sqrt{\frac{T_{acc}}{\tau_R}} D_{\max}}$$

Consistent with the relation inferred from laboratory experiments by Ohnaka and Yamashita 1989.
Their theoretical and numerical results start from the crack model assumption, not including the local healing of slip. Our assumptions are completely different, but the inferred relations are consistent.

$$\boxed{V_{peak} \propto C(V_r)\Delta\tau_b}$$

Resolution of dynamic parameters

Which is the resolution of our models?
We want to verify the actual capability in measuring *Dc*!

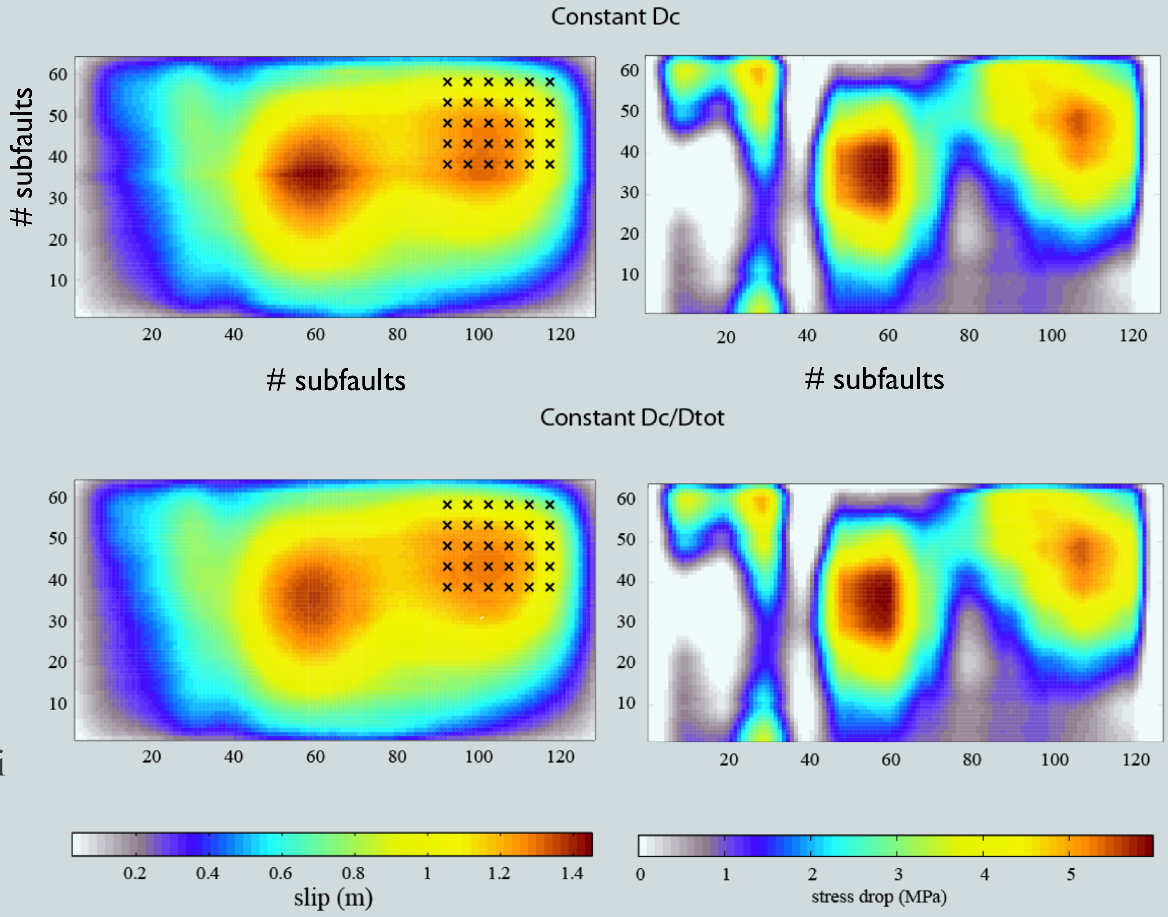

Two slip distribution of 2000 Western Tottori event inferred from a dynamic modeling by assuming Constant Dc or Constant Dc/Dtot.

Resolution of dynamic parameters

Model 2:
Spontaneous dynamic rupture model with constant Dc

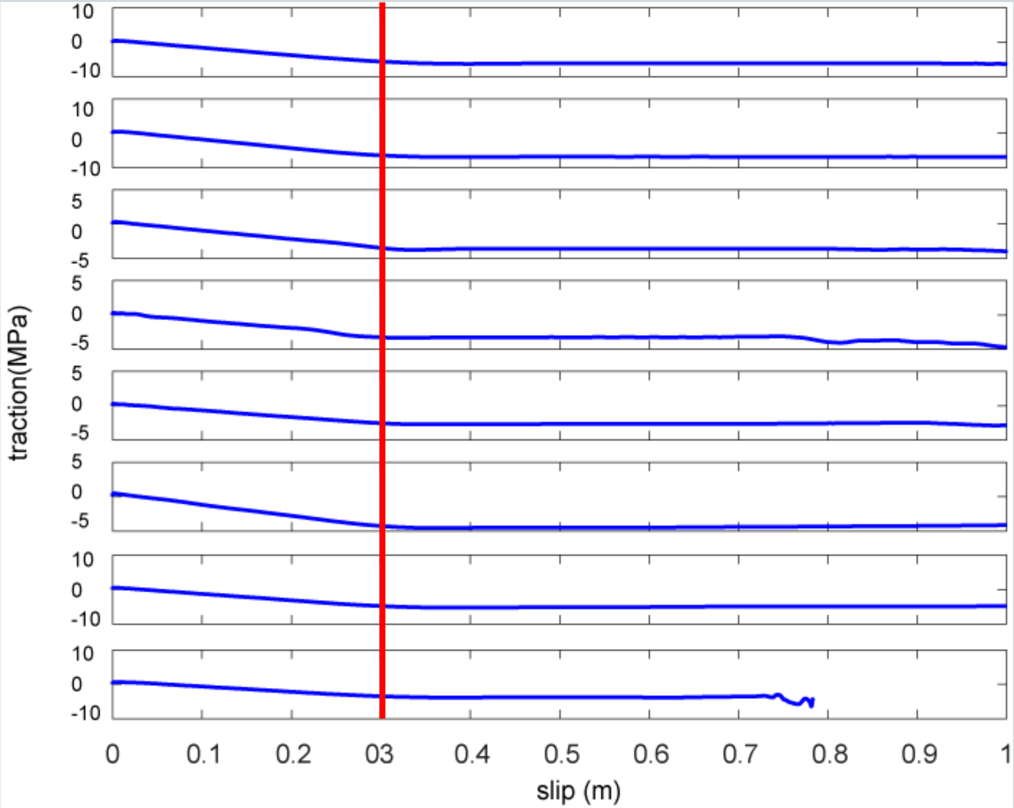

Examples of traction versus slip curves at several target points. Dc is 0.3m everywhere.

Resolution of dynamic parameters

Model 3:
Spontaneous dynamic rupture model with constant Dc/Dtot spatial distribution on the fault plane.

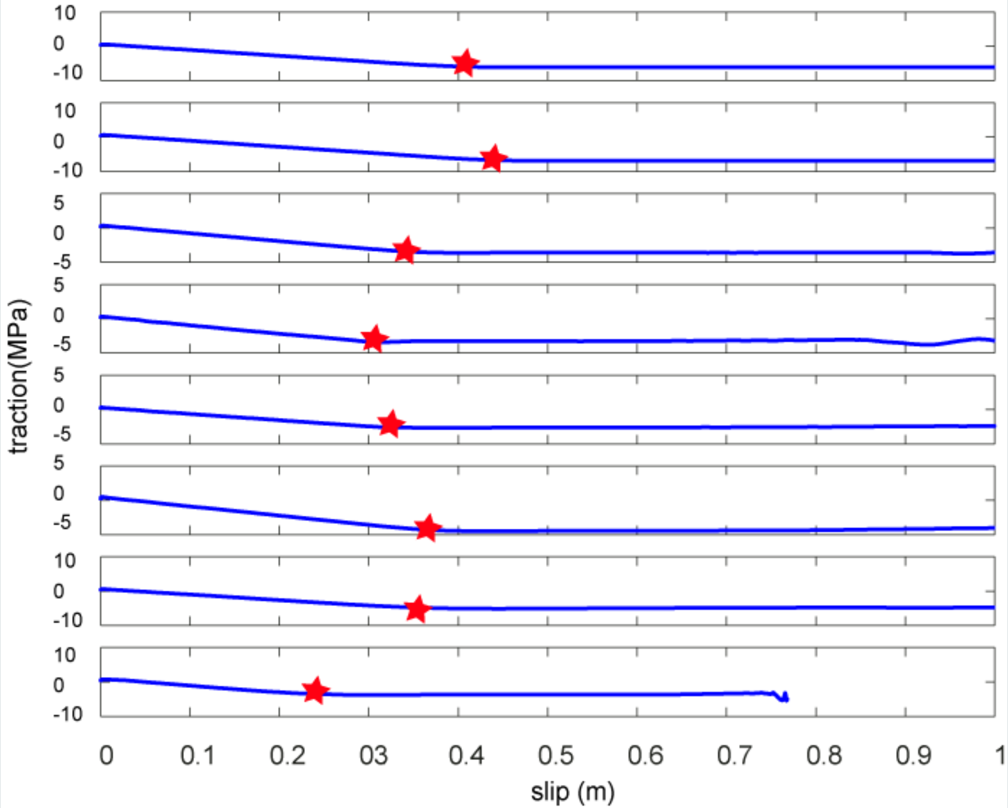

Examples of traction versus slip curves at several target points. Range of Dc distribution:

0.1m-0.45m

Resolution of dynamic parameters

Slip velocity evolutions

Dc constant

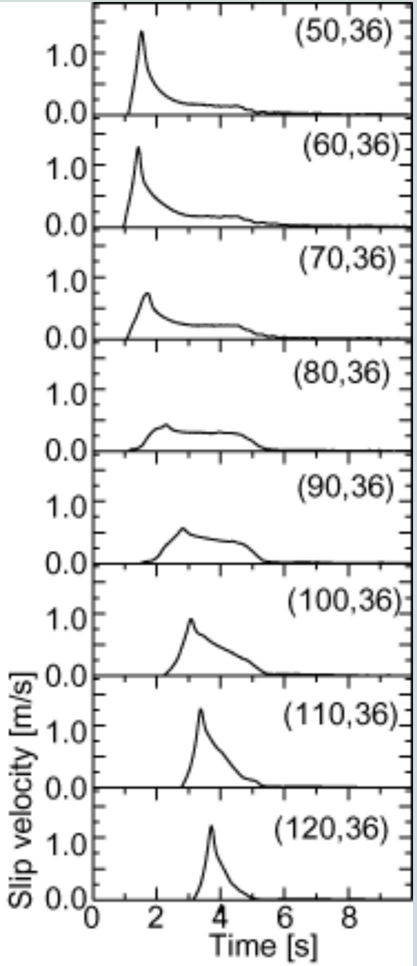

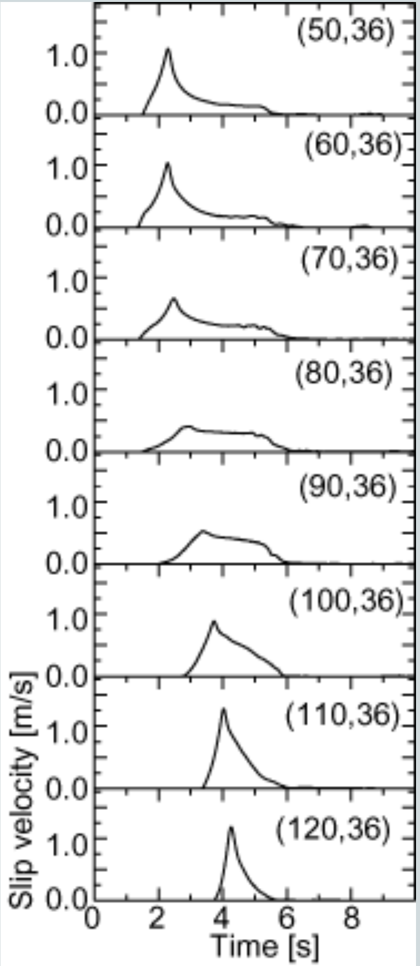

D_c/D_{max} constant

Resolution of dynamic parameters

-Are we able to infer the "true" dynamic parameters from the slip velocity evolutions?

-Can we distinguish between dynamic models with constant Dc (i.e., heterogeneous Dc/Dmax) and constant Dc/Dmax (i.e., heterogeneous Dc)?

-In the heterogeneous model, is still valid the empirical relation relating kinematic and dynamic parameters ?

$$D_c \propto \sqrt{\frac{T_{acc}}{\tau_R}} D_{\max}$$

Resolution of dynamic parameters

STRATEGY:

• The original dynamic models represent the "true" models.

• We fit the original slip velocity histories with the Yoffe function (described with D_{max}, T_{acc} and t_R). [synthetics data]

• We compute the dynamic evolution using Yoffe function as a boundary condition.

•We compare the inferred traction evolution and Dc values along the fault plane with the original Slip Weakening behavior

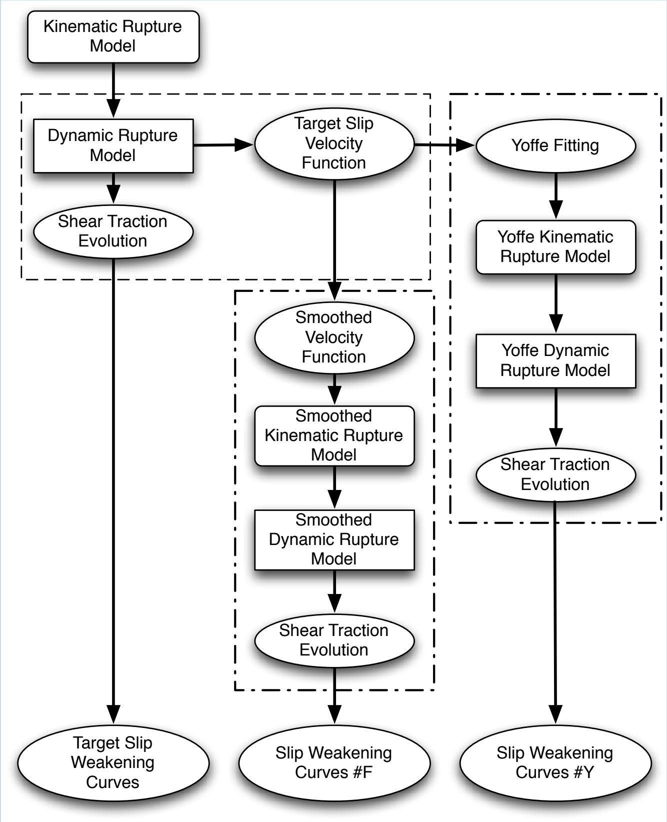

Resolution of dynamic parameters

RED=original slip velocities;

BLUE= best fit for the three parameters with the interpolation tecnique

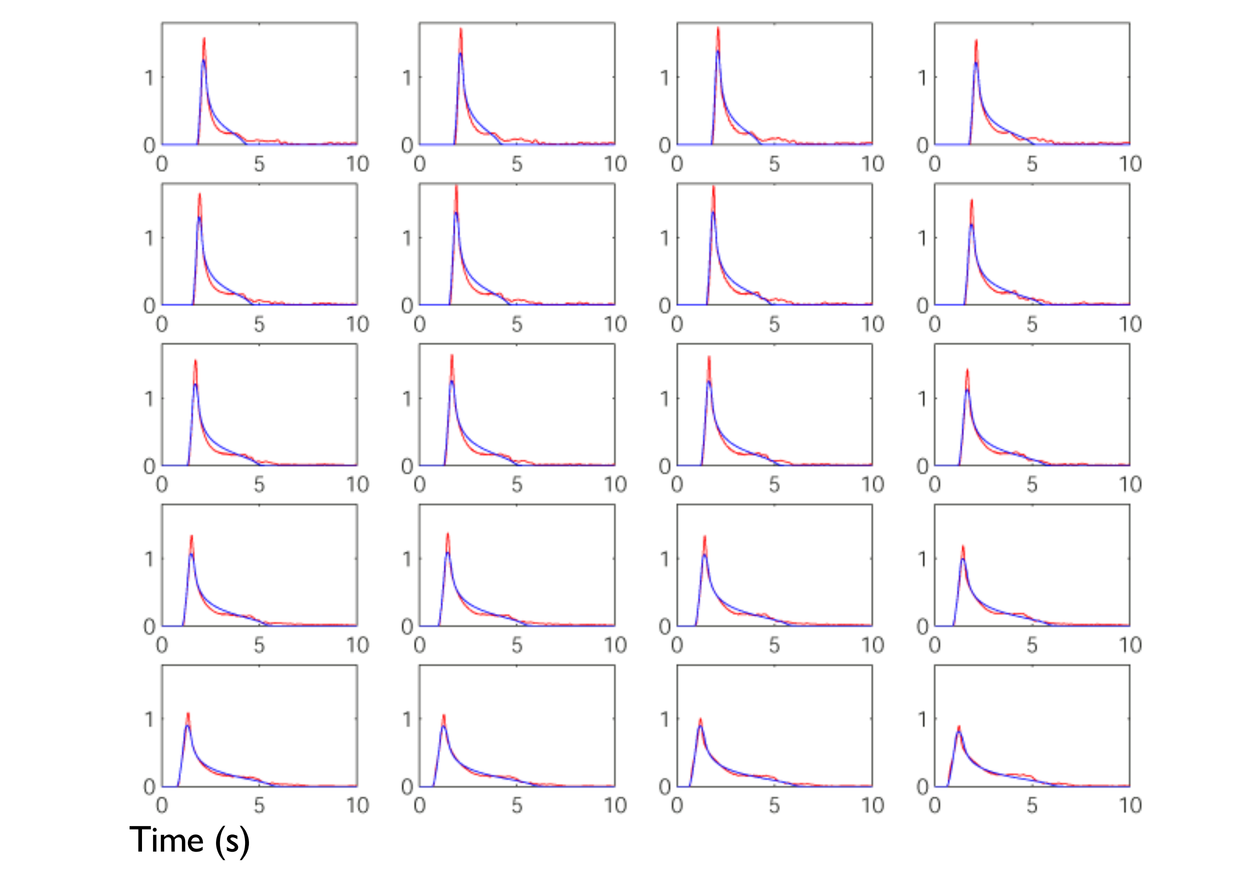

Resolution of dynamic parameters

RED=original traction evolution;

BLUE= retrieved traction evolution

Our numerical tests show that fitting the slip velocity functions of the target models at each point on the fault plane for the model with Constant Dc is not enough to retrieve good traction evolution curves and to obtain reliable measures of D_c.

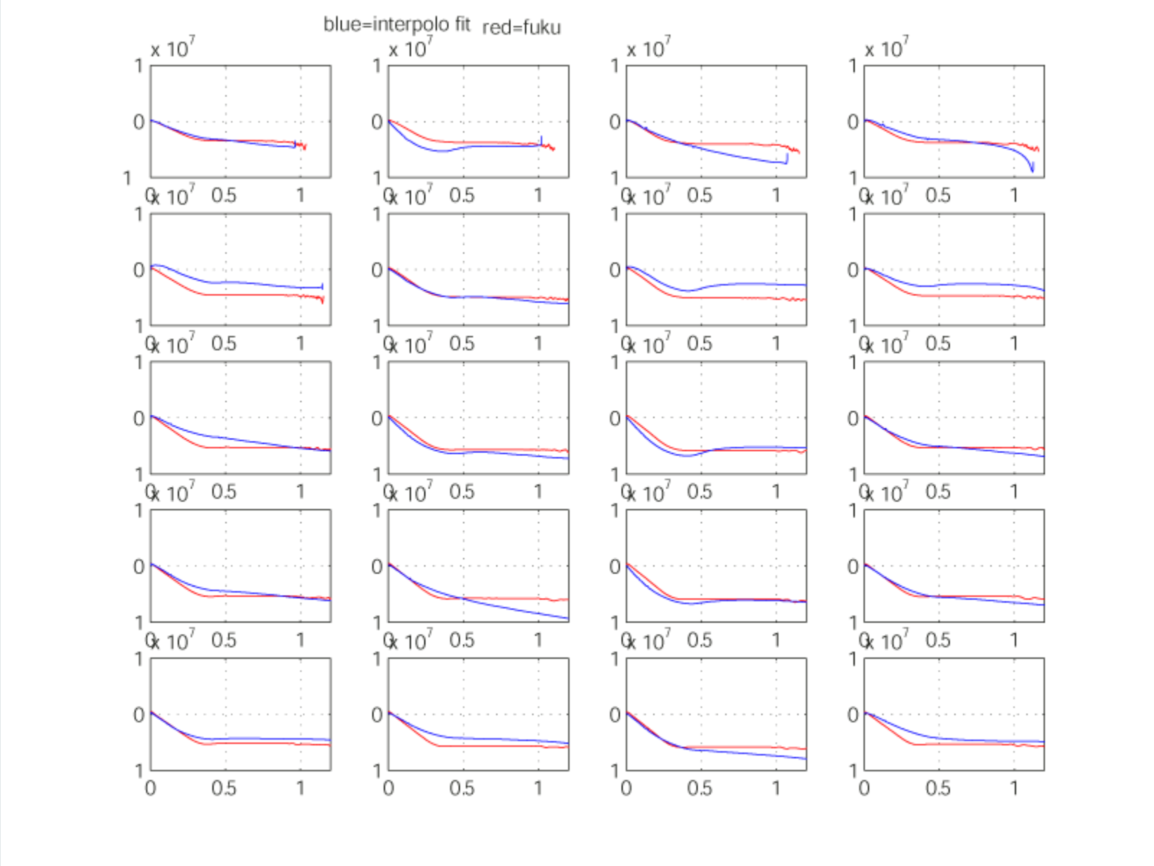

Resolution of dynamic parameters

Constant Dc

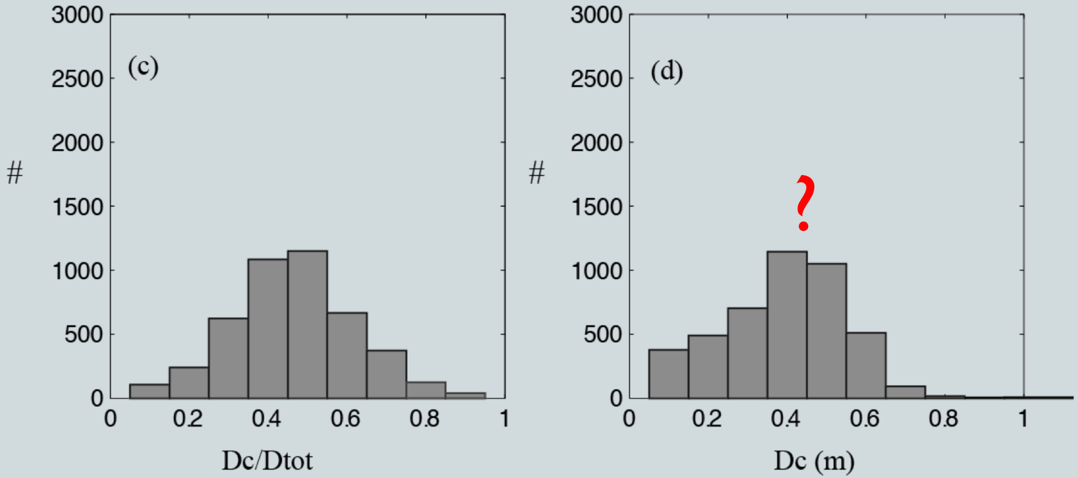

Constant Dc/Dtot

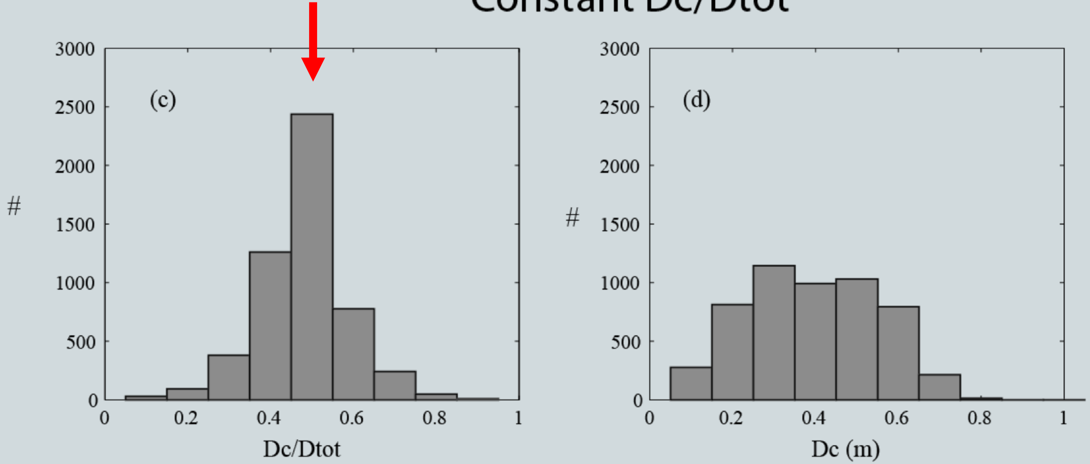

Resolution of dynamic parameters

- The results of this study confirm that the adopted numerical procedure provides correct dynamic traction evolution when the slip history is perfectly known. However, any small modification to the real source time function affects the estimate of *Dc*.

- The estimation of Dc is very sensitive to any small variation of the slip velocity function.

- The inferred *Dc*/*D*tot ratio from the best-fitting Yoffe functions is quite reasonably imaged, although slightly overestimated.

- An artificial correlation between Dc/Dtot is obtained when a fixed shape of slip velocity is assumed on the fault (i.e. constant rise time and constant time for positive acceleration, mimic the common ignorance on the duration of the positive slip acceleration) which differs from that of the target model.

- The estimation of fracture energy (breakdown work) on the fault is not affected by biases in measuring Dc.

Dc’ estimates

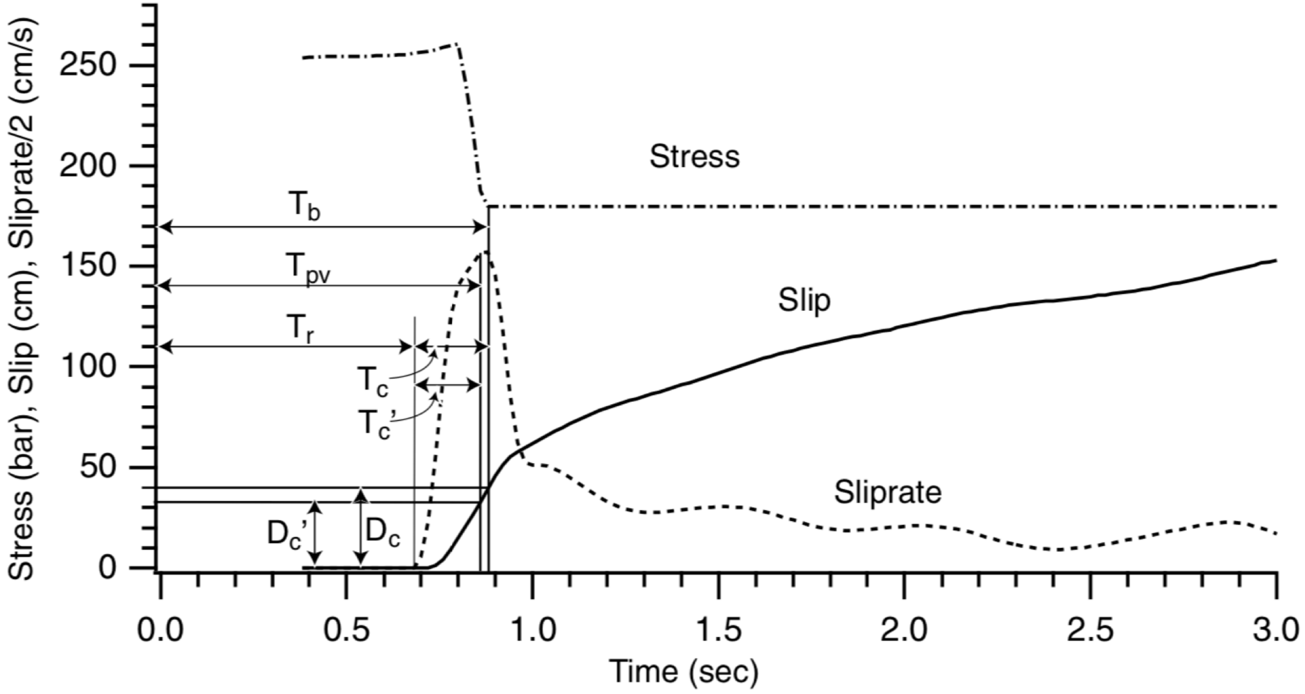

Figure 3. A typical behavior of the time history of shear stress, slip, and slip velocity on the fault. T_b, breakdown time of stress; T_{pv}, time of peak slip-velocity; D_c, slip at time T_b; D_c', slip at time T_{pv}.

Near-fault deformation and Dc″ during the 2016 Mw7.1 Kumamoto earthquake

Eiichi Fukuyama* and Wataru Suzuki

Abstract

An Mw7.1 Kumamoto earthquake occurred at 01:25:05 on April 16, 2016 (JST). The earthquake involved a rupture at a shallow depth along a strike-slip fault with surface breaks. Near-fault ground motion records, especially those of a strike-slip earthquake, can provide us with direct information on the earthquake source process. During the earthquake, near-fault seismograms were obtained at KMMH16 station located about 500 m off the fault. The ground displacements were well recovered from the double numerical integration of accelerograms at KMMH16 both on the surface and at the bottom of the 252-m-deep borehole. Fault-parallel static displacement was estimated to be about 1.1 m from the acceleration waveforms. The Dc″ value, which is defined as double the fault-parallel displacement at peak velocity time, was proposed as a proxy of the slip-weakening distance. Using both the velocity and displacement fault-parallel waveforms, the Dc″ value was estimated at about 1 m. This value was between 30 and 50% of the total slip on the fault, which is consistent with previous observations.

Keywords: Near-fault displacement, Slip-weakening distance, Strike-slip fault

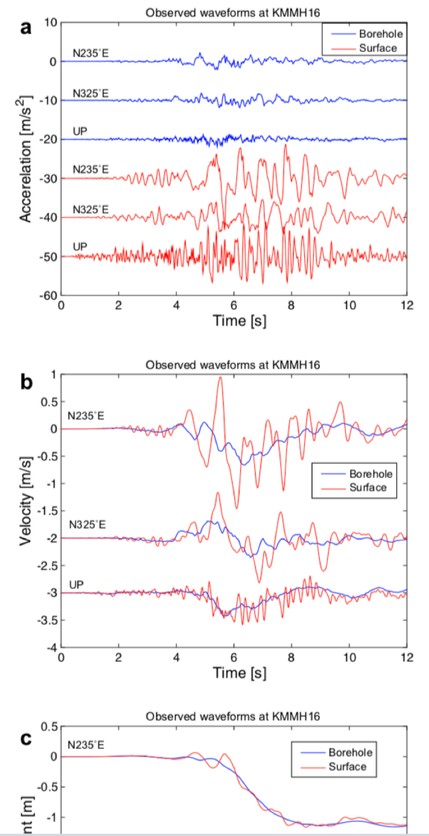

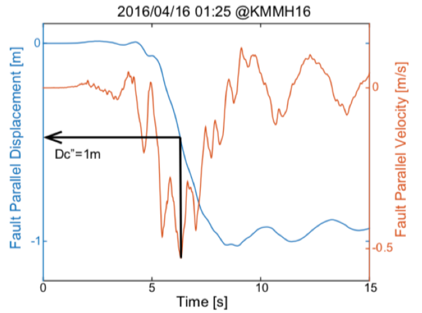

Fig. 4 Fault-parallel velocity and displacement at KMMH16 are plotted for the estimation of the Dc″ value

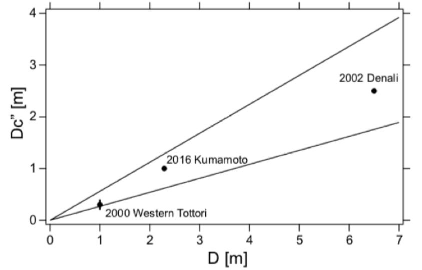

Fig. 5 Comparison between the final slip D and estimated Dc″ values for the 2000 Western Tottori earthquake estimated at GSH station, the 2002 Denali at PS10 station and the 2016 Kumamoto at KMMH16 station. *Two solid lines* stand for the upper and lower limits of Dc (Dc″ = 0.56 D and Dc″ = 0.27 D, respectively) estimated by Mikumo et al. (2003). Modified from Fig. 4 of Fukuyama and Mikumo (2007)

Kinematic source inversions provide a framework for incorporating observational constraints into earthquake rupture models, and in principle allow for independent estimation of finite-fault stress parameters that can be compared to standard earthquake source studies based on point- source assumptions.

kinematic inversion models (of limited resolution) may carry useful information on the scaling of dynamic source properties

Average measures of stress drop and breakdown work (seismological fracture energy)

Source Heterogeneity: how much of source complexity is translated into radiated ground motion variability ?

We can average local estimates of stress drop on different fault portions. These different average values yield a variability up to a factor 5 in stress drop

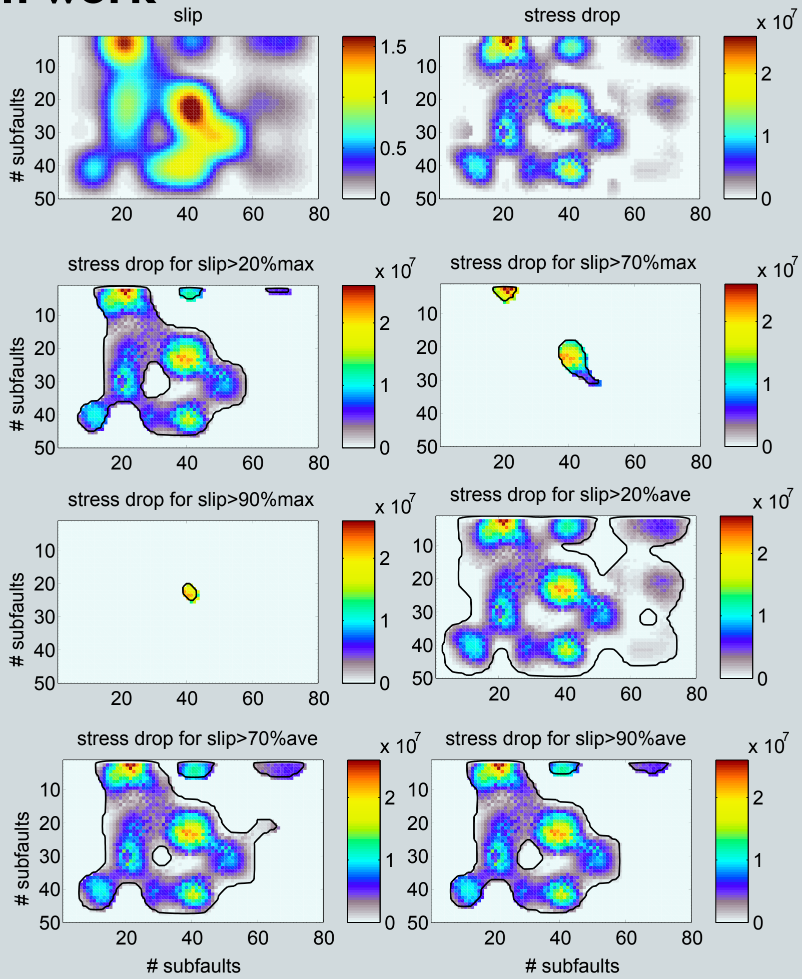

Average measures of stress drop and breakdown work (seismological fracture energy)

Average W_b over region of fault having slip > 20% of average slip

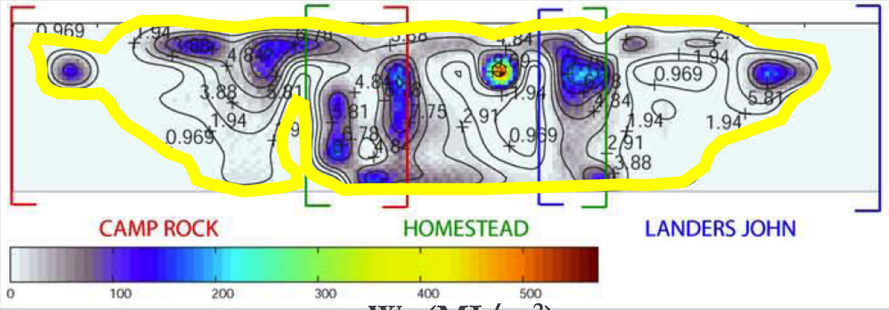

W_b (MJ/m^2)

Average W_b over region of fault having slip > 70% of maximum slip

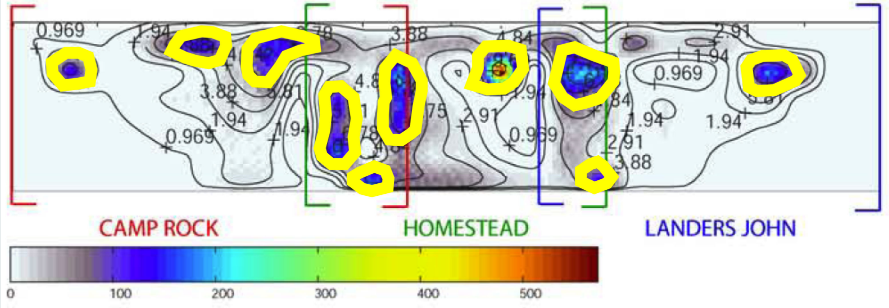

W_b (MJ/m^2)

Two estimates of average Wb for a kinematic rupture model of Landers

Average measures of stress drop and breakdown work (seismological fracture energy)

Seismological Fracture energy (breakdown work) scaling with slip

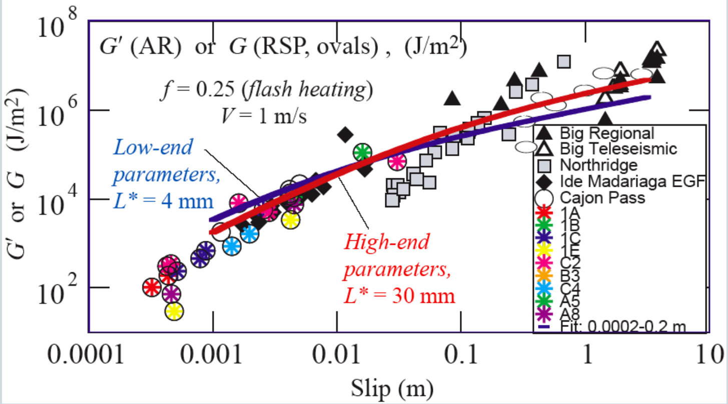

Abercrombie & Rice 2005

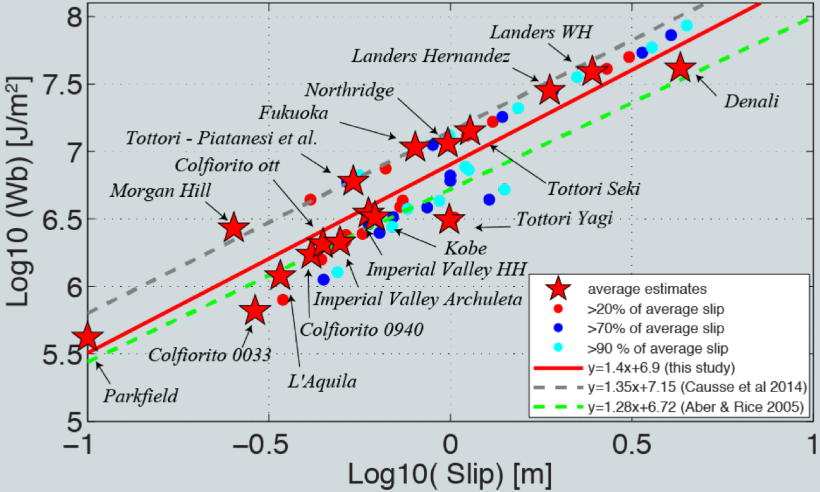

Breakdown work (or fracture energy) scales with seismic moment following a power law whose slope is nearly 0.6.

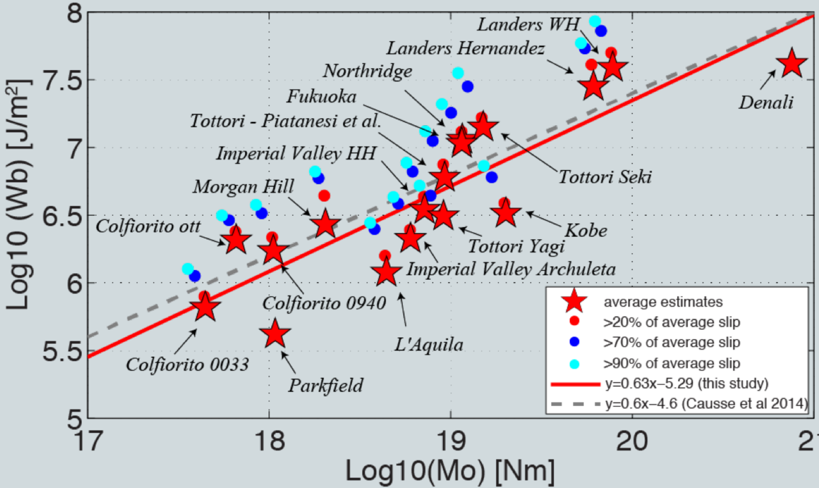

Average measures of stress drop and breakdown work (seismological fracture energy)

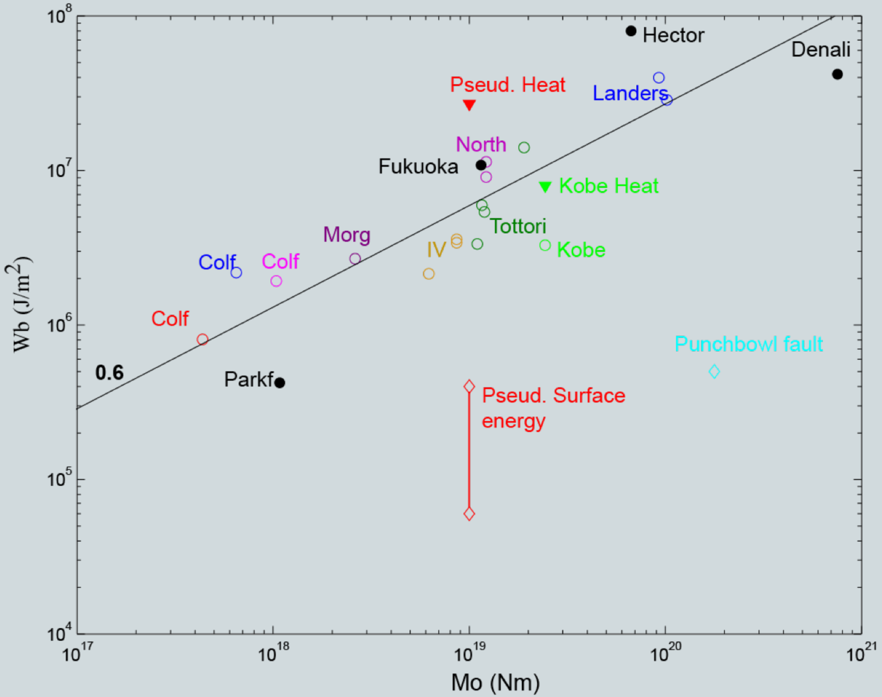

The comparison between geologic measurements of surface energy and breakdown work revealed that 1-10% of breakdown work went into the creation of fresh fracture surfaces (surface energy) in large earthquakes, and the remainder went into heat.

Average measures of stress drop and breakdown work (seismological fracture energy)

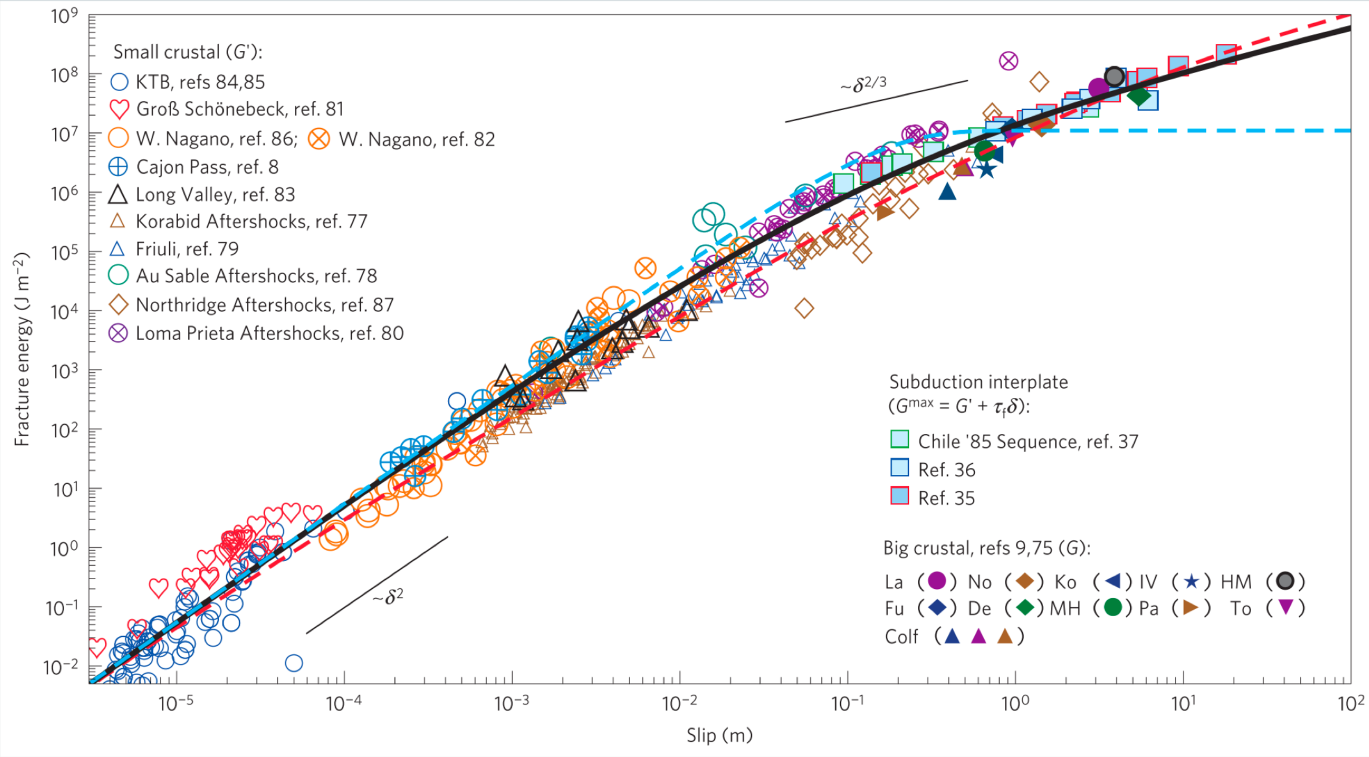

Viesca and Garagash (2015)

They observe a distinct transition in how fracture energy scales with event size, which implies that faults weaken differently during small and large earthquakes, and earthquakes are not self-similar.

They found that for small slip, the early time undrained-adiabatic deformation results in fracture energy scaling as $G \propto \delta^2$, and for large slip, where shear heating resembles slip on a plane, $G \propto \delta^{2/3}$

Average measures of stress drop and breakdown work (seismological fracture energy)

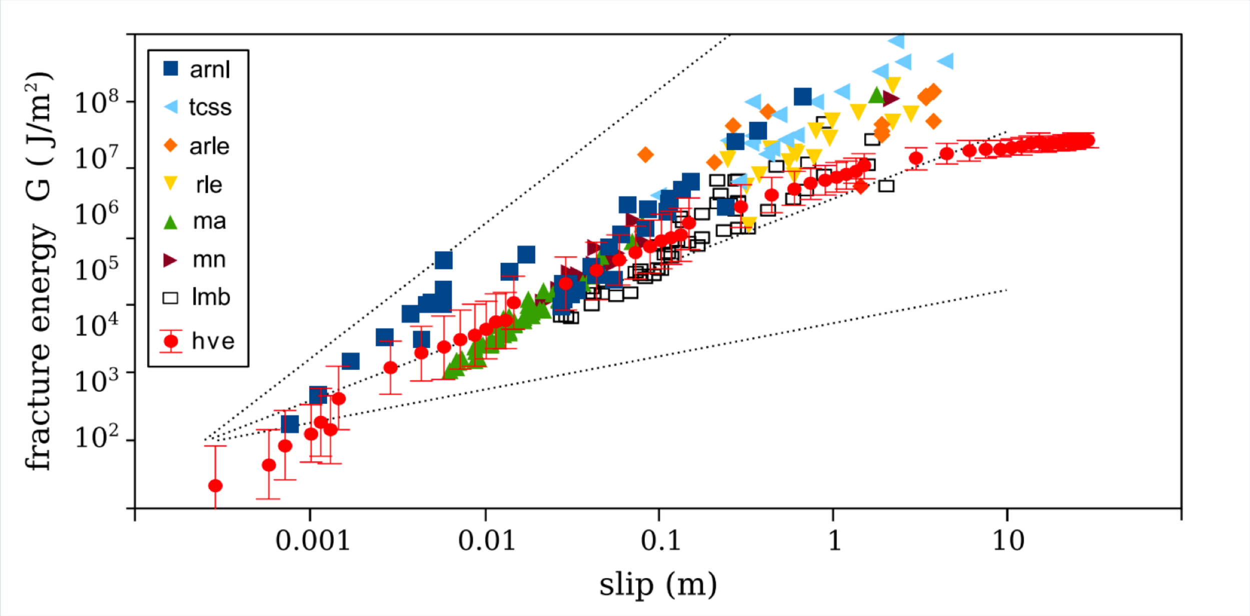

- Scaling of lab data is coherent with that of seismological observations
- Curvature at high slip values might depend on termo- / poro-elastic processes
- High velocity friction experiments involve mechanical work similar to seismological estimates

Nielsen et al 2016

Breakdown work scaling with slip: average or peak slip estimates

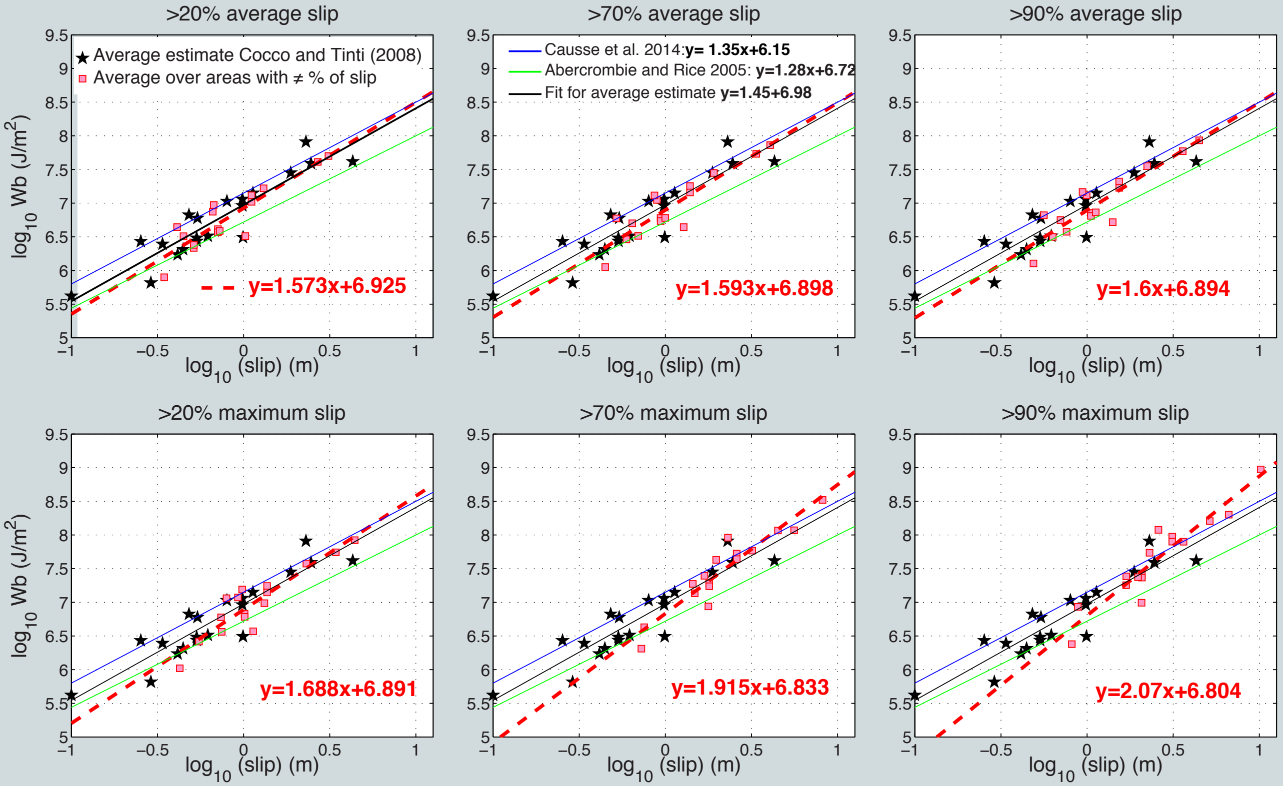

Stress drop scaling with seismic moment

- Stress drop varies over 3 decades in amplitude for a large range of seismic moment
- Individual sequences seem to show trend of increasing stress drop with earthquake size

Averaged from Extended sources

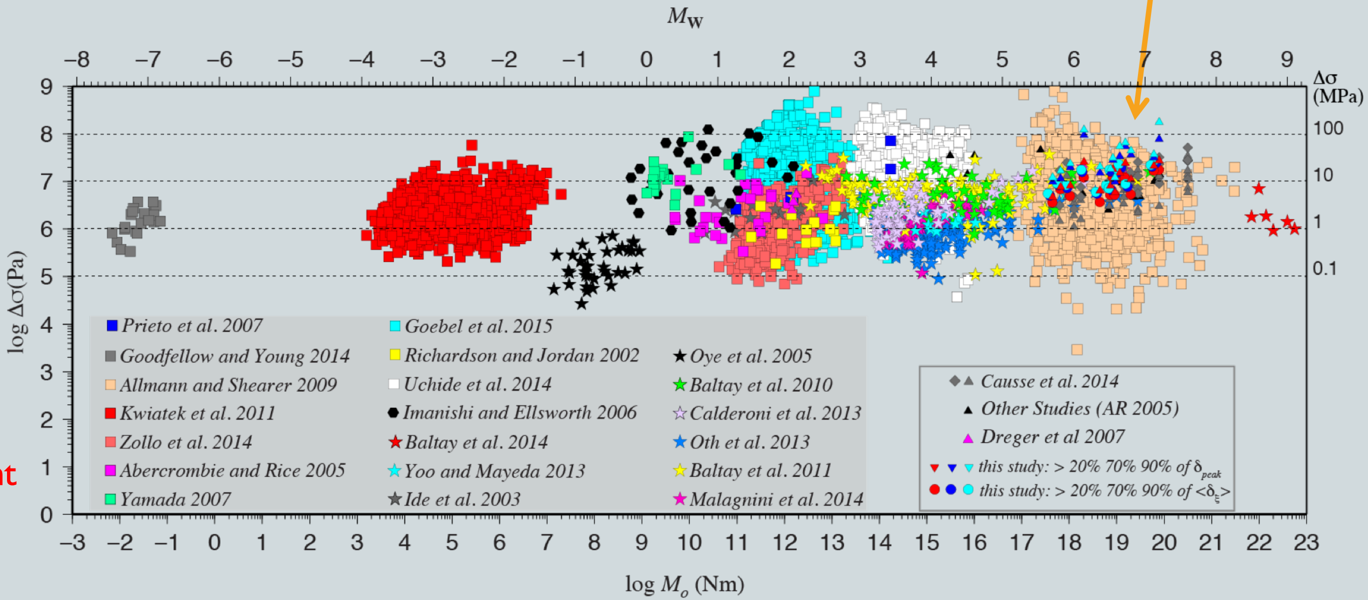

Estimated from point source models

- Seismological results cannot provide any information on the governing micro-scale physical processes. They can provide the estimate of the macroscopic frictional work absorbed during dynamic fault weakening
- A common feature in mechanics of dynamic shear rupture propagation is that unstable failure is associated with dynamic fault weakening represented by the traction evolution with time or slip
- Wb is a reliable parameter while Dc is model dependent.
- Slip velocity contains all information to model earthquake dynamics. Find relieable slip velocity is a challenge!

Open questions and future work

- New Dynamic inversion procedures
- Validate if kinematic models are dynamically consistent
- Link with laboratory experiments to real events to infer/validate slip velocities and constitutive laws

Physical intuition of scale dependence

fracture + friction = Dynamic weakening

Different physical mechanisms can control dynamic weakening each of which has its own spatial and temporal length scales

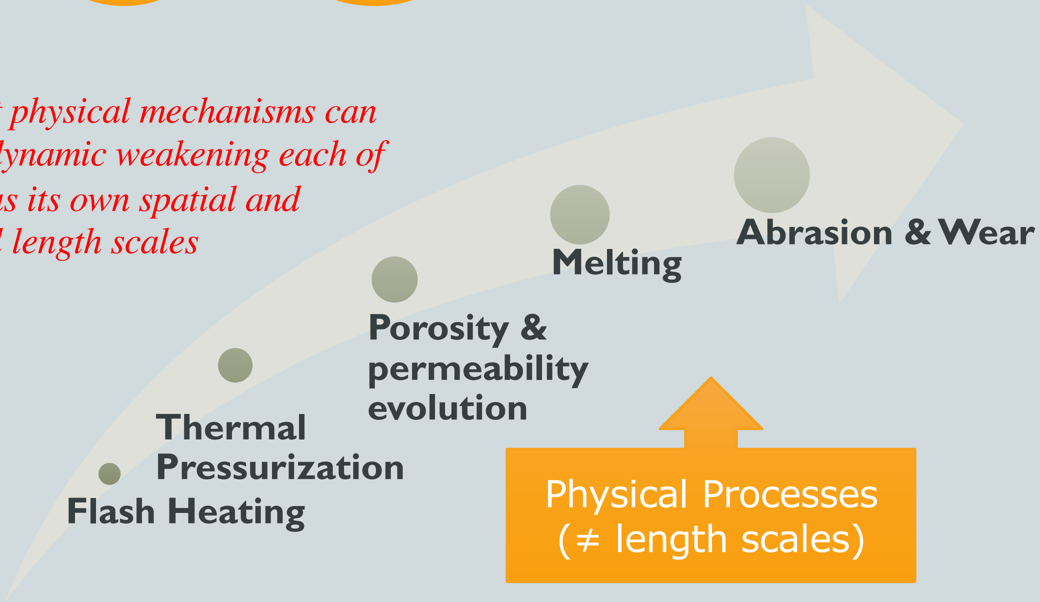

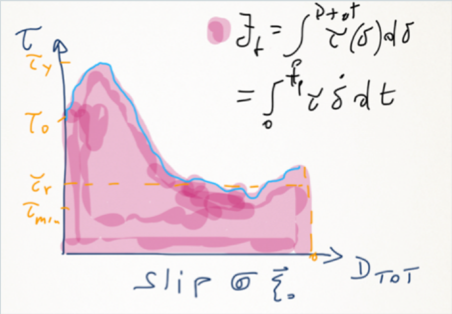

Physical Processes (≠ length scales)

Outcome of scale dependent processes Multi-scale weakening

We need a next generation of laboratory derived constitutive laws, which will allow us to study individual physical processes and understanding scale dependence

Scale Dependence

- The mathematical representation of dynamic fault weakening implies scale dependence:
  - Fault zone thickness, h (h ~ 10 m ÷ 1 km)
  - Slipping zone thickness, h_S (h_S ~ 10 μm ÷ 1 cm)
  - Propagating slipping zone size, L (L ≈ h)
  - Breakdown zone size, R (R ≤ L)
  - Seismic wavelengths of interest (λ ≈ 0.1 ÷ 1 km)
  - Roughness of the principal slipping surface (λ_c≈μm÷mm)
  - Dimension of asperity contacts (≈ μm÷m)

Length scale parameters

- Scale dependent fault parameters characterizing dynamic fault weakening:
  - Fracture Energy (G)
  - Stress drop (breakdown, dynamic, static stress drops)
  - Critical Slip Weakening distance D_c
  - Fault Strength (Σ)

Laboratory experiments

Slip velocity is poorly known, although it contains all information to model earthquake dynamics. Constraining slip rate is a key challenge.

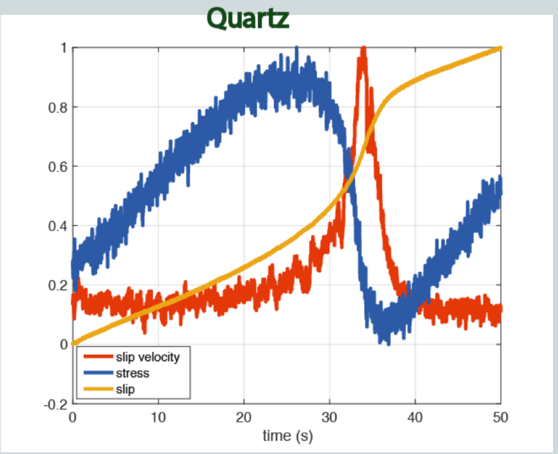

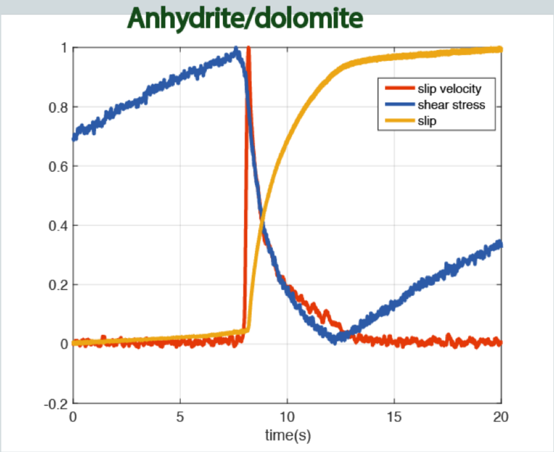

Traction, slip and slip velocity evolutions for laboratory seismic cycles by using two different materials: Quarzt and Anhydrite/Dolomite

Reconciling seismological measurements, geological observations and the key findings of laboratory experiments

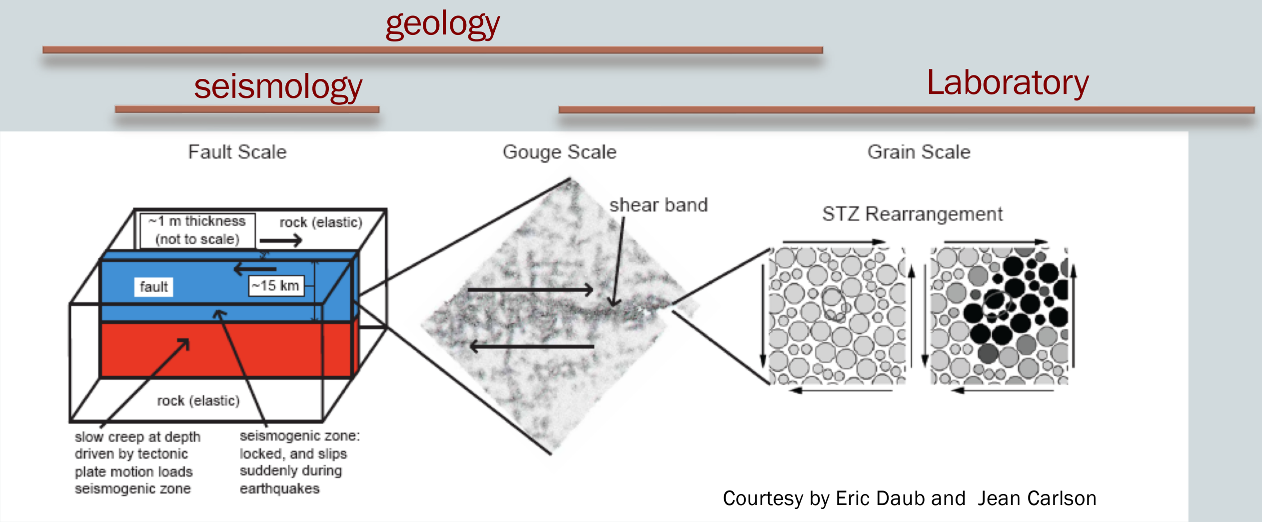

Daub, E. G., and J. M. Carlson, Friction, Fracture, and Earthquakes, Ann. Rev. Cond. Matter Phys. 1, 397-418 (2010).

The present challenge in earthquake source mechanics is reconciling seismological measurements, geological observations and laboratory experiments in order to obtain a coherent understanding of the governing physical processes.

Open questions Dynamic traction evolution

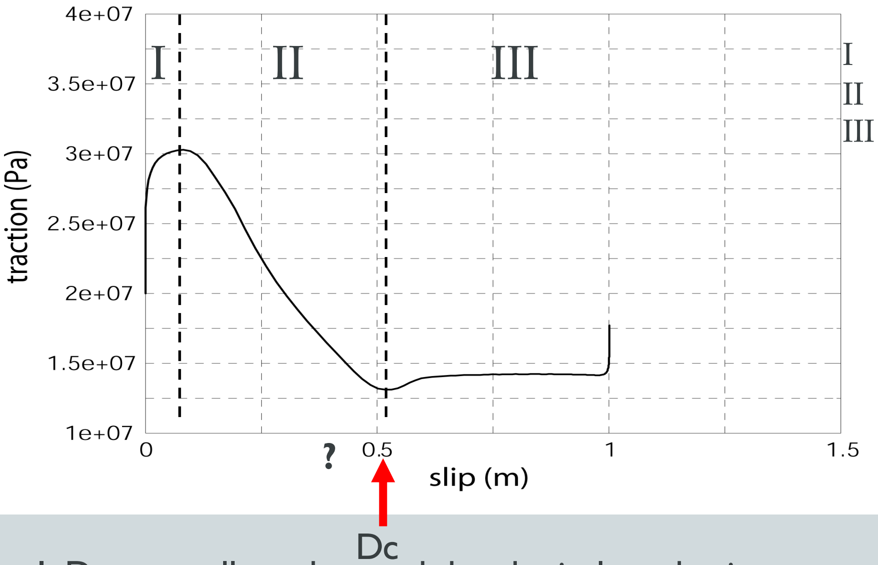

I – hardening ↔ dynamic loading
II – weakening ↔ stress drop
III – restrengthening ↔ healing of slip

1. Do we really understand the physical mechanisms controlling the dynamic traction evolution?

2. Which is the actual size of the critical slip weakening distance?

3. Do we really know the slip velocity time function and its evolution during the propagation of a dynamic crack? The resolution of kinematic models and the choice of the source time function affect the calculation of dynamic traction evolution.